Science of the Total Environment 789 (2021) 148006

Contents lists available at ScienceDirect

Science of the Total Environment

journal homepage: www.elsevier.com/locate/scitotenv

A case study using 2019 pre-monsoon snow and stream chemistry in the Khumbu region, Nepal

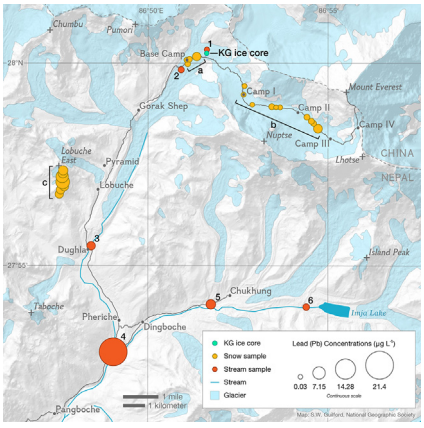
Heather M. Clifford [a,b,*], Mariusz Potocki [a,b], Inka Koch [c,d], Tenzing Sherpa [c], Mike Handley [a], Elena Korotkikh [a], Douglas Introne [a], Susan Kaspari [e], Kimberley Miner [a], Tom Matthews [f], Baker Perry [g], Heather Guy [h], Ananta Gajurel [i], Praveen Kumar Singh [c,j], Sandra Elvin [k], Aurora C. Elmore [k], Alex Tait [k], Paul A. Mayewski [a]

[a] Climate Change Institute, University of Maine, ME, USA
[b] School of Earth and Climate Sciences, University of Maine, ME, USA
[c] International Centre for Integrated Mountain Development, Lalitpur, Nepal
[d] Department of Geosciences, University of Tübingen, Tübingen, Germany
[e] Department of Geological Sciences, Central Washington University, WA, USA
[f] Department of Geography and Environment, Loughborough University, Loughborough, UK
[g] Department of Geography and Planning, Appalachian State University, NC, USA
[h] School of Earth and Environment, University of Leeds, UK
[i] Central Department of Geology, Tribhuvan University, Kathmandu, Nepal
[j] CoEDMM, Indian Institute of Technology Roorkee, Roorkee, Uttarakhand, India
[k] National Geographic Society, 1145 17th St. NW, Washington, DC, USA

HIGHLIGHTS

- Document chemical composition of snow, stream, and ice from Khumbu region, Nepal
- Provide a framework for future monitoring of environmental chemistry
- Characterize chemical signatures in snow and stream chemistry
- Provide evidence for elevated levels of human-sourced metals in snow and streams
- Increased tourism in the Khumbu are likely contributors to high metal concentrations

GRAPHICAL ABSTRACT



ARTICLE INFO

Article history:
Received 21 January 2021
Received in revised form 11 May 2021
Accepted 20 May 2021
Available online 25 May 2021

Editor: Thomas Kevin V

ABSTRACT

This case study provides a framework for future monitoring and evidence for human source pollution in the Khumbu region, Nepal. We analyzed the chemical composition (major ions, major/trace elements, black carbon, and stable water isotopes) of pre-monsoon stream water (4300–5250 m) and snow (5200–6665 m) samples collected from Mt. Everest, Mt. Lobuche, and the Imja Valley during the 2019 pre-monsoon season, in addition to a shallow ice core recovered from the Khumbu Glacier (5300 m). In agreement with previous work, pre-monsoon aerosol deposition is dominated by dust originating from western sources and less frequently by transport from southerly air mass sources as demonstrated by evidence of one of the strongest recorded pre-monsoon events emanating from the Bay of Bengal, Cyclone Fani. Elevated concentrations of human-sourced metals (e.g., Pb, Bi,

* Corresponding author at: Sawyer Environmental Research Building, University of Maine, Orono, ME 04469, USA.
E-mail address: heather.clifford@maine.edu (H.M. Clifford).

https://doi.org/10.1016/j.scitotenv.2021.148006
0048-9697/© 2021 The Author(s). Published by Elsevier B.V. This is an open access article under the CC BY license (http://creativecommons.org/licenses/by/4.0/).

Keywords:
Mt. Everest
Pollution
Climate change
Glacier
Human impacts
Heavy metals

As) are found in surface snow and stream chemistry collected in the Khumbu region. As the most comprehensive case study of environmental chemistry in the Khumbu region, this research offers sufficient evidence for increased monitoring in this watershed and surrounding areas.

© 2021 The Author(s). Published by Elsevier B.V. This is an open access article under the CC BY license (http://creativecommons.org/licenses/by/4.0/).

1. Introduction

Glaciers and snow cover in high mountain regions play a significant role in regional hydrology and ecology (Immerzeel et al., 2020). In the Himalayas, modern environmental stresses such as climate change are causing a decline in glacier volume and an increase in the risk of glacier outburst floods (Wang et al., 2019). The Khumbu Glacier, as with almost all Himalayan glaciers, is in a state of negative mass balance (Bolch et al., 2012; King et al., 2017), leading to increased melt. Long-term projections of amplified melt, in combination with other changing climatic factors like precipitation patterns, indicate increased pressure on water availability and food security for rural Himalayan communities (Wang et al., 2019). Meltwater from local glaciers such as the Khumbu Glacier is responsible for ~65% of the local domestic water supply during the dry, pre-monsoon season (Wood et al., 2020). The local population of 3500–6000 people in the Khumbu region depends on stream water for their drinking, irrigation, and ecological purposes (Wood et al., 2020). Additionally, around 57,000 trekkers, climbers, and local support teams make the trek to Everest Base Camp annually (Government of Nepal, 2020), with several thousand climbers seasonally residing at Everest Base Camp, depending upon the local streams derived from Khumbu Glacier melt for drinking/cooking.

Down-glacier residents face a seemingly contradictory threat from glacier outburst floods and freshwater decline due to warming and accelerated melt (Pritchard, 2019). Further melt is also associated with wind-blown debris lowering glacier surface albedo (Hansen and Nazarenko, 2004; Kaspari et al., 2014). In addition, and most relevant to this study, as snow and glaciers melt, entrapped chemicals are released that are both essential to ecosystems and agriculture (Immerzeel et al., 2020) and in some cases detrimental (King et al., 2017; Miner et al., 2020) to ecosystems and human health. Precipitation and melt can contain toxic substances associated with distant sources such as fossil fuel combustion and metal production and local activities such as agriculture and biomass burning.

Asia is the most significant global contributor of atmospheric anthropogenic trace metals (Pacyna and Pacyna, 2001). While heavy metals occur naturally, anthropogenic activity results in significantly higher levels in the atmosphere, which can be detrimental to human health. Long-distance heavy metals and soot sources can include land usage, mining, metal smelting, oil, and coal combustion. Local sources for the Khumbu region include leaded aviation fuel for helicopters, generators, dung burning, batteries, and local incinerators (Elvin et al., 2020). Whether natural or anthropogenically sourced, enhanced concentrations of heavy metals in the environment globally are of concern to human health (Fernández-Luqueño et al., 2013; Mishra et al., 2014; Mohod and Dhote, 2013; Tchounwou et al., 2012).

Long-range transport and deposition of aerosols in the Himalayas are strongly influenced by the seasonal migration of the South Asian monsoon, with comparatively greater accumulation of aerosols during the non-monsoon season, compared with the monsoon season (Bonasoni et al., 2012; Carrico et al., 2003; Cong et al., 2009; Duan et al., 2009; Kang et al., 2007). Chemical fingerprinting of air masses illustrates the distinct differences between Tibetan Plateau (cold, dusty) and Indo-Gangetic (warm, marine, with anthropogenic and biogenic inputs) source air masses (Mayewski et al., 1980). Differences between seasonal summer monsoon and winter precipitation chemistry in Himalayan ice cores thus reflect changes in air mass source. Source variability for instance leads to high dust content (e.g., Ca^{2+}, Mg^{2+}, SO_4^{2-},NO_3^-) in pre-monsoon layers and a strong marine (Na^+, Cl^-) signal in monsoon layers (Kang et al., 2004, 2002, 1999; Marinoni et al., 2001; Mayewski et al., 1983, 1980; Wake et al., 1993). Whereas pre-monsoon precipitation shows a strong influence from the prevailing westerlies, originating over North Africa and the Middle East before they pass over India to Nepal, monsoon season air transport is dominated by southern air masses from the Bay of Bengal (Cong et al., 2009; Perry et al., 2020).

The chemical composition of atmospherically-deposited aerosols in snow can be used to track air mass pathways, along with source and emission strength for certain chemical components (Balestrini et al., 2016; Cong et al., 2010b, 2010a; Grigholm et al., 2015; Kang et al., 2007; Shrestha et al., 2002). The chemical signatures can be compared to instrumented climate records revealing proxies for past regional climate and atmospheric composition from snow pits and ice cores (Shichang et al., 2002; Wake et al., 1993, 1990). For example, recent increases in anthropogenically sourced aerosols (e.g., heavy metals, black carbon) in the Himalayas can be associated with both long-distance transport, as well as increased local anthropogenic activities, including agriculture, expansion in land use, and biomass burning (Cong et al., 2010a; Jenkins et al., 1995; Kaspari et al., 2014, 2009b; Reynolds et al., 1995; Stone et al., 2010). Black carbon deposition, which is highest during the pre-monsoon season and likely to be transported via valley winds, is predominantly associated with regional (Nepal and India) and western sources, likely from the Middle East (Gul et al., 2021; Marinoni et al., 2010). Specific to the Khumbu region, a baseline of atmospheric chemical signatures are provided by atmospheric research from the Nepal Climate Observatory at Pyramid (e.g., Bonasoni et al., 2008; Decesari et al., 2010; Jacobi et al., 2015; Marinoni et al., 2010) and surface snow studies on major ions and trace elements (e.g., Balestrini et al., 2016, 2014; Marinoni et al., 2001; Valsecchi et al., 1999).

Pioneering work on water (e.g., streams, lakes) chemistry in the Khumbu region determined the weathering influence from complex bedrock geology and presence of debris-ridden moraines, while evidence of agricultural activities was detected at lower altitudes (Jenkins et al., 1995; Reynolds et al., 1995; Tartari et al., 1998b). The growing tourism population in the Khumbu (quadrupled since 1995) has become increasingly detectable via human and animal waste chemical and bacterial signatures (Ghimire et al., 2013a, 2013b, Nicholson et al., 2016, 2019) in waterways, especially in lower elevation, pre-monsoon surface waters. Pursuing research in remote, high mountain regions, such as the Khumbu, is logistically challenging (e.g., Elvin et al., 2020), causing difficulty in collecting the necessary information to complete long-term or widespread studies. With this case study, we contribute further investigations necessary to fill gaps in scientific knowledge, such as details in the chemical signatures of atmospheric conditions during the shoulder seasons like the pre-monsoon, anthropogenic influences on atmospheric deposition in the Khumbu region, and how the chemistry in the watershed can be affected by increased glacier melt, local and distant anthropogenic influences, and changes in precipitation seasonality.

To construct a framework of environmental chemistry during the late pre-monsoon period in the Khumbu region, we present the chemical composition (major and trace elements, major ions, black carbon, and stable water isotopes) of surface snow, stream, and an ice core

collected (Fig. 1) as part of the 2019 National Geographic and Rolex Perpetual Planet Everest Expedition. The main objectives for this case study are: 1) to expand current understanding on the spatiotemporal deposition of chemicals by investigating pre-monsoon snow and stream chemistry, 2) to determine background chemistry from a shallow ice core comprising ice from dated prior to 1950, 3) to develop a profile of chemical characteristics for a pre-monsoon storm that resulted in significant snow accumulation, and 4) to characterize the state of anthropogenic pollution in snow and streams in the Khumbu region. To our knowledge, this is the first characterization of chemistry extracted from Khumbu Glacier ice and the first detailed characterization of pre-monsoon snow/water elemental chemistry for the region.

2. Methods

2.1. Study area

The study area (Fig. 1) is located in the Khumbu and Imja Valley regions in Sagarmatha National Park, Nepal, between 27.8676 and 28.0205°N and 86.7569 and 86.9391°E. The boundary of our study area begins on the southern trail to Mount Everest- known locally as Sagarmatha and Chomolungma- at the Dingboche (4410 m) and Pheriche (4370 m) villages and continues to Everest Base Camp (30 km away; ~5300 m) on the Khumbu Glacier, then continues up the climbing route toward Mt. Everest summit, as far as Camp II (6665 m). The extent of Everest Base Camp for this study, as observed during the 2019 climbing season, is defined as between 28.0048°N; 86.8566°E and 27.9962°N; 86.8483°E.

The pre-monsoon period (March to May) in the Khumbu Valley region is defined by well-developed south-eastern up-valley breeze with high wind speed and gusts, which weaken toward the end of May, with the onset of the south-western monsoon (Tartari et al., 1998a). Up-valley (anabatic) winds are dominant during the day-time and periods of precipitation while down-valley (katabatic) winds are more prevalent during the night and early morning (Bonasoni et al., 2010). Annually averaged daily wind speed from Pyramid automatic weather station (AWS) for 1994–1996 (Tartari et al., 1998a) is 1.39 m/s, with the highest wind strength (gusts exceeding 38 m/s) during winter and lowest in the post-monsoon (October–November), while pre-monsoon wind speed ranges from about 3 to 8 m/s (based on 2006–2007 measurements by Bonasoni et al. (2010)).

Minimum annual temperatures occur during winter (~−15 °C daily min.) and maximum annual temperatures occur during the summer monsoon (~8 °C daily max.), while annually, daily mean values range between about 5 to −10 °C based on 1994–1999 AWS data at Pyramid (Bollasina et al., 2002). The pre-monsoon season is defined by high solar radiation, with a mean temperate of −2.9 °C with mean diurnal ranges of 10.2 °C, and temperatures increasing from the winter minimum to summer maximum (Tartari et al., 1998a). Precipitation in the Khumbu region is concentrated in the monsoon season, which is accountable for 76% of annual precipitation, while only 17% occurs during the pre-monsoon season (Perry et al., 2020).

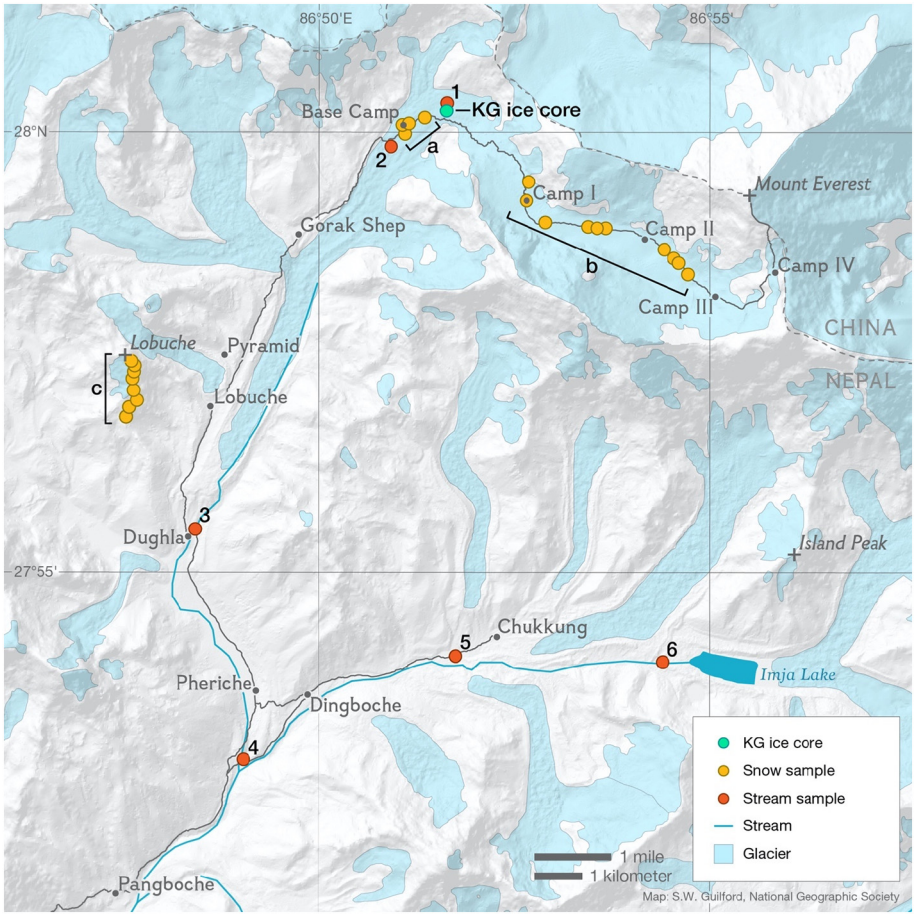


Fig. 1. Sample map from the Khumbu region, Nepal. Shaded map of the regional area with location of snow (yellow), stream (red), and ice core samples (black), as well as the current glacial extent (aqua), stream paths (turquoise), and main trekking and climbing routes (gray). Snow sample group locations identified as the following: a) Basecamp, b) Camp I,II, and c) Mt. Lobuche. Stream sample locations identified as the following: 1) KGM1, 2) KGM2, 3) Dughla, 4) Pheriche, 5) Chukkung, and 6) Imja. Glacial extent is sourced from the 2018 GLIMS glacier database (Raup et al., 2007), and polygons for the Everest area glaciers are extracted from the 2014 GLIMS dataset. Figure created by Sam Guilford.

During the study period (2019/04/17 to 2019/05/10), temperatures ranged from −9 to 8 °C (average temperature of −1.1 ± 3.7 °C), wind speed ranged from 0.1 to 6.5 m/s (average 2.3 ± 1.6 m/s), relative humidity ranged from 14 to 100% (average 76 ± 23%), and 35 mm w.e. of total precipitation fell over the 26 days, taken from hourly meteorological data from the Pyramid Weather Station (27.959°N, 86.813°E; 5035 m). During this period, there were two major precipitation events (>10 mm) with high relative humidity, 16–17 April and 3–4 May (Cyclone Fani storm event), while other notable precipitation events (>0.5 mm) occurred on 22, 23, and 30 April. No wind direction data is available for the study period from the local weather stations the authors had access to.

2.2. Sample collection

2.2.1. Ice core samples

This study's ice core was collected from the Khumbu Glacier (28.0039°N, 86.8583°E, 5300 m), about 300 m east of Everest Base Camp west of the Khumbu icefall (Fig. 1), using a modified Kovacs Mark III drilling system with a 7.25 cm core diameter and powered by a Milwaukee hand drill. The core was collected to provide a baseline for pre-anthropogenic era chemistry records from the immediate sampling area for comparison with the modern samples collected in this study. We collected a total of 3.5 m of ice, which was analyzed for major ions, trace elements, and stable water isotopes at the University of Maine Climate Change Institute. Aerosol-based micro-radiocarbon dating of the ice core sections was conducted using the top and bottom 0.9 m of ice (1.8 m total), following the procedure described in Uglietti et al. (2016), with sample processing at the Paul Scherrer Institute and radiocarbon analysis at the Laboratory for the Analysis of Radiocarbon with AMS of the University of Bern, Switzerland.

2.2.2. Surface snow samples

A total of 94 surface snow samples were collected from Everest Base Camp, Mt. Lobuche, and the Mt. Everest climbing route up to 6665 m between April 14, 2019, to May 10, 2019 (Fig. 1; Table S1). To collect the surface snow, DI-rinsed 250 mL HDPE containers were used, according to the cleaning procedure detailed in Dixon et al. (2011). Extreme care and protective gear (e.g., polyethylene gloves) were used to assure the samples were not contaminated. All samples were collected from the upper ~5 cm of snow, immediately sealed, and stored in a sampling tent at Everest Base Camp. Due to the length of the field season, there was no viable way to keep the 250 mL sample containers frozen in the field, therefore, the samples were allowed to melt after collection. Snow samples for black carbon analysis were collected in smaller 50 mL containers and stored frozen in vacuum thermoses and portable freezers. All samples were flown to Kathmandu via helicopter, where they were stored until shipping to the University of Maine (Elvin et al., 2020).

At Everest Base Camp (~5300 m), samples were collected almost daily ($n = 63$) from three locations (Sites 1, 2, 3) and from an additional site (Site 4) immediately following the Cyclone Fani event (described further in Section 3.3). Site 1 was located close to the multiple caravans of tents in the Everest Base Camp, on the debris-covered Khumbu Glacier, ~50 m away from the closest tent. Sites 2 and 3 were ~ 100 m away from tents and located between the penitentes on the Khumbu Glacier. Site 4 was located within the camp, about 5 m from the closest tent. Immediately following Cyclone Fani, we collected 24 fresh snow samples on the morning of May 4th ~ 1000 NPT, from Sites 1, 2, and 4. Camp I and II samples were collected along the southern climbing route, from ~100 m west of the tents at Camp I (6000 m) up to the Western Cwm (western side valley), and Camp II (6665 m). From Mt. Lobuche climbing route ($n = 7$), surface snow was collected every 100 m in elevation up to the summit (~5400–5900 m) on May 1st, following a >1.1 mm snow event (29–30 April based on observations at a local weather station located at Pyramid).

2.2.3. Stream samples

To determine the chemical composition of surface waters in the Khumbu region, we sampled six locations along the Khumbu Glacier meltwater stream, Khumbu Valley streams, and Imja valley streams (Fig. 1, Table S1). We collected three replicate samples at each location (18 samples total), sampled directly from the surface (top 5 cm) of the running streams using the same cleaning, storage, and shipping procedures detailed in Section 2.2.2. The upper Khumbu Glacier melt stream samples were collected from a meltwater stream located northwest of the Khumbu icefall and south-east of Everest Base Camp (~250 m from the closest tents). The lower Khumbu Glacier melt stream samples were collected from a meltwater stream within the crevasse ridges, located about 200 m directly south and downslope of the farthest tents on the southwest side of Everest Base Camp, closest to the entry to the trekking path. The Khumbu Valley samples, fed by meltwater from the Khumbu Glacier, and Mts. Pumori, Chumbu, and Lobuche were collected from two meltwater stream locations, one located ~150 m northwest of the Dughla settlement, and the other ~1200 m downstream from the Pheriche village. The Imja Valley samples, fed predominantly by the Imja Glacier, were collected from two stream locations, one located at the outlet of Imja lake and the other collected ~1000 m downstream from the Chukkung village.

2.3. Chemical analysis

Prior to analysis, the snow and stream samples were siphoned into three volumes: 5 mL in Dionex™ AS-DV autosampler polyvials with filter caps for ion chromatography (IC), 5 mL in glass bottles with Phenolic PolyCone Lined Caps for stable water isotope analysis, and the remaining volume was acidified to 1% with Optima double-distilled HNO_3 and left to digest for 60 days prior to ICP-SFMS analysis. To analyze the Khumbu Glacier ice core, we used a continuous melting system resulting in ~200 samples (~0.85 cm resolution), detailed in Osterberg et al. (2006). To assure no contamination from the drill or during transport influenced the chemistry, the inner portion of the ice core is melted and siphoned for IC and ICP-SFMS analysis, while the outer portion of the core is melted and siphoned for stable water isotope analysis.

Snow, stream, and ice samples were analyzed for major ions, major/trace elements, and stable water isotopes using instruments and techniques located at the University of Maine's Climate Change Institute. The seven major ions (Ca^{2+}, Na^{+}, Mg^{2+}, K^{+}, NO_3^-, SO_4^{2-}, Cl^-) were analyzed using a Thermo Scientific™ Dionex™ Ion Chromatograph ICS-6000 analytical system fitted with suppressed conductivity detectors and Dionex AS-HV autosampler. The 48 major/trace elements (Ag, As, Al, B, Ba, Bi, Ca, Cd, Ce, Co, Cr, Cs, Cu, Dy, Er, Eu, Fe, Gd, Ho, K, La, Li, Lu, Mg, Mn, Mo, Na, Nd, Ni, P, Pb, Pr, S, Sb, Sc, Si, Sm, Sr, Tb, Th, Ti, Tm, U, V, W, Y, Yb, Zn) were analyzed using a Thermo Electron Element 2 Inductively Coupled Plasma Sector Field Mass Spectrometry (ICP-MS) coupled to a Cetac Model ASX- 260 autosampler. A summary of blank measurements and detection limits for ICP-MS and IC data of ice core and snow/stream samples are presented in Table S2 and Table S3, respectively. Analysis of blank measurements and detection limits signifies that there is negligible sample contamination for the snow, stream, and Khumbu Glacier ice core ICP-MS and IC measurements used in this study during collection, transport, and chemical analyses. We removed two samples from Everest Base Camp from this study that skewed the data as outliers which were assumed to be contaminated, potentially caused by a bad seal or undetected crack in the sample container. Contamination is assumed for these two samples from Everest Base Camp due to more than three elements having concentrations >0.99 percentile, and for one Cyclone Fani sample with Cu values 7000% greater than the average. The stable water isotope measurements ($\delta^{18}O$, δD), reported as per mil relative to Standard Mean Ocean Water (SMOW), were analyzed as vapor on a Picarro Laser Cavity 109 Ringdown Spectrometer (Model L2130-i) with a high throughput vaporizer. Based on various analyses of internal and international

standards, the long-term precision is 0.1‰ (1σ) for $\delta^{18}O$ and 0.4‰ (1σ) for δD.

Snow samples for black carbon were shipped frozen and analyzed at Central Washington University. The samples were melted in a warm water bath, sonicated, and agitated with a magnetic stir bar during sample measurement. Samples were subsequently nebulized using a Marin-5 nebulizer and coupled to an extended range single-particle soot photometer (SP2) to measure refractory black carbon. Measured concentrations were calibrated using Aquadag standards and all samples were blank corrected.

3. Results

3.1. Ice core chemistry

Ice core samples preserve the signature of past conditions, therefore to estimate past atmospheric composition in the region, we sampled and analyzed the chemistry from the 3.5 m deep ice core drilled from the Khumbu Glacier (28.0039°N, 86.8583°E, 5300 m), directly below the Khumbu icefall (Fig. 1). Aerosol-based micro-radiocarbon dating (Uglietti et al., 2016) of the top and bottom sections yielded ages of 1040 ± 161 yr cal BP at the top of the core and 196 ± 128 yr BP (before 1950) at the bottom, suggesting that the section of collected ice was rotated in its descent down the icefall. Here we define modern as years after 1950. Since the sample resolution for this ice core is likely an average of multi-annual values, the comparison with modern pre-monsoon snow samples is not straightforward, nevertheless, the chemistry in this ice provides an estimate of pre-modern concentrations that can be compared with modern snow and stream sampling data.

We compare the average concentrations of selected chemistry from the Khumbu Glacier ice core, snow, and stream samples from this study (Fig. 2), specifically major crustal elements (Si, Fe, Al, Mg, Ca), major marine ions (Na^+, Cl^-), anions (SO_4^{2-}, NO_3^-), and known anthropogenically-influenced elements (Pb, U, As, Bi, Cs) (Casey, 2012; Cong et al., 2010a; Dong et al., 2015; Gabrielli et al., 2020; Jiao et al., 2021; Kaspari et al., 2009b; Lee et al., 2008; Tripathee et al., 2014a). Additional chemistry measurements and statistics are included in the supplementary material (Fig. S1, S2; Table S2). The most abundant elements (>1% total concentration) measured within the Khumbu Glacier ice core are as follows: Si > Ca > S > Fe > Al > Mg > P > Na > K. For ions, Ca^{2+} makes up 76% of the total cation concentration and SO_4^{2-} makes up 64% of the total anion concentration, followed by $Na^+ > K^+ > Mg^{2+}$ and $NO_3^- > Cl^-$. The Khumbu Glacier ice core has generally depleted $\delta^{18}O$ values, compared with snow and stream averages, ranging from −13.8 to −24‰ (average − 21.2‰). This range aligns with $\delta^{18}O$ values measured from ice cores drilled on the northern side of Mt. Everest (Zhang et al., 2005) and from Dasuopu, both in Tibet (Thompson et al., 2000), most likely reflecting variability in the strength of the Indian summer monsoon and source of precipitation.

Principal component analysis (PCA) of the Khumbu Glacier ice core chemistry, summarized in Table S4, reveals predominantly crustal and marine sources. To investigate source regions, a PCA was applied to the chemistry in the snow, water, and ice samples, using the sci-kit (v0.20.2) module in Python 3.6. PCA is used to reduce the dimensionality of the measured sample chemistry, allowing identification of patterns or relationships. The analysis includes all major ions and all trace elements, except rare earth elements as well as Mo, Sb, Cd, and Ag due to their low concentrations. Crustal elements from dust dominate the first principal component ($PC1_{ice}$; 40%) (e.g., Fe, Al, K, Mg, Ti, Ba, V, Si). $PC2_{ice}$ (21%) is largely composed of SO_4^{2-}, S, Ca^{2+}, Ca, Sr, As, U, Mg^{2+}, possibly due to solutes from the rock debris confined in the ice core (Takeuchi et al., 2020). $PC3_{ice}$ (8%) is dominated by marine source ions (Na^+, Cl^-), in addition to Zn, Na, K^+, and Cu. In $PC1_{ice}$ and $PC2_{ice}$ (40% and 21% variance, respectively) crustal elements likely originate from southern/central Asia and the Tibetan Plateau (Kang et al., 1999, 2004, 2007; Kaspari et al., 2007, 2009a; Wake et al., 1993) and localized dust sources, respectively (Balestrini et al., 2014; Casey, 2012; Casey et al., 2012; Reynolds et al., 1995). $PC3_{ice}$ for Khumbu Glacier ice core (8% variance) is dominated by marine source chemistry (Cl^-, Na), potentially derived from southerly sources that dominate during the monsoon season and are less frequent during the pre-monsoon season (Perry et al., 2020; Valsecchi et al., 1999). The average Na^+/Cl^- ratio (0.84) in this ice core is close to that found in seawater (0.86), indicating a marine or possibly evaporite source (**Fig. S3, S4**).

3.2. Snow chemistry

To analyze the potential role and spatial distribution of anthropogenic pre-monsoon sources to the Khumbu region, we measured major ions, trace elements, and stable isotopes in 94 snow samples, collected from three general locations in the Khumbu Valley (Fig. 1): Everest Base Camp (~5250 m, $n = 39$), Camp I and Camp II (6026–6665 m, $n = 24$) and Mt. Lobuche (5280–5875 m, $n = 7$). These locations were chosen because of the accessibility from trekking routes and varying elevations. We collected an additional 24 samples from snow accumulation at Everest Base Camp during 3–4 May 2019,

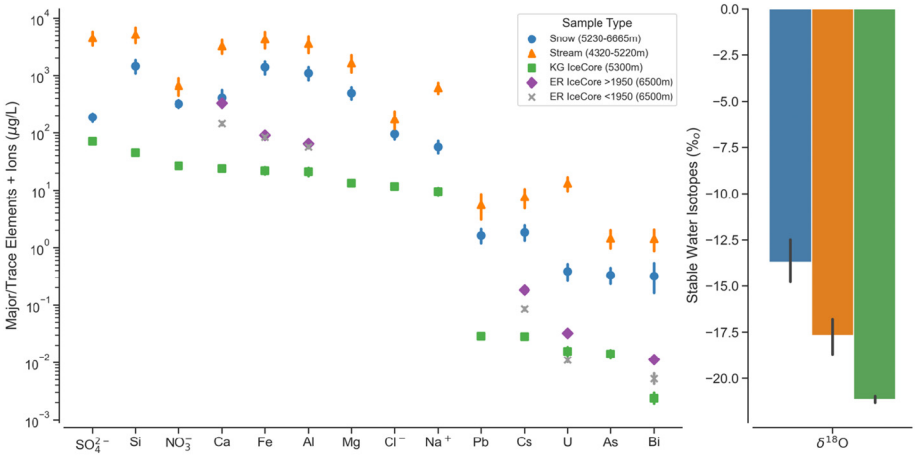


Fig. 2. Overview of Snow, Streams and Ice Chemistry. Average total concentrations of selected chemistry from snow (blue circles, $n = 94$), stream (orange triangles, $n = 18$), Khumbu glacier ice core (green square, $n = 200$), East Rongbuk ice core 1950–2002 (purple diamond, n = 859, Kaspari et al. (2009b)) and East Rongbuk ice core 1650–1950 (gray 'x', $n = 1352$, Kaspari et al. (2009b)) samples in ascending order of average ice core concentrations for crustal (Si, Fe, Al, Mg, Ca), marine (Na^+, Cl^-), anions (NO_3^-, SO_4^{2-})and known anthropogenically influenced chemistry (Pb, U, As, Bi, Cs). Isotopic variations in the air mass tracer $\delta^{18}O$ are shown on the right for snow (blue), stream (orange) and Khumbu Glacier Ice Core (green). All error bars show 95% confidence intervals. Extended chemistry measurements are found in Supplementary Material.

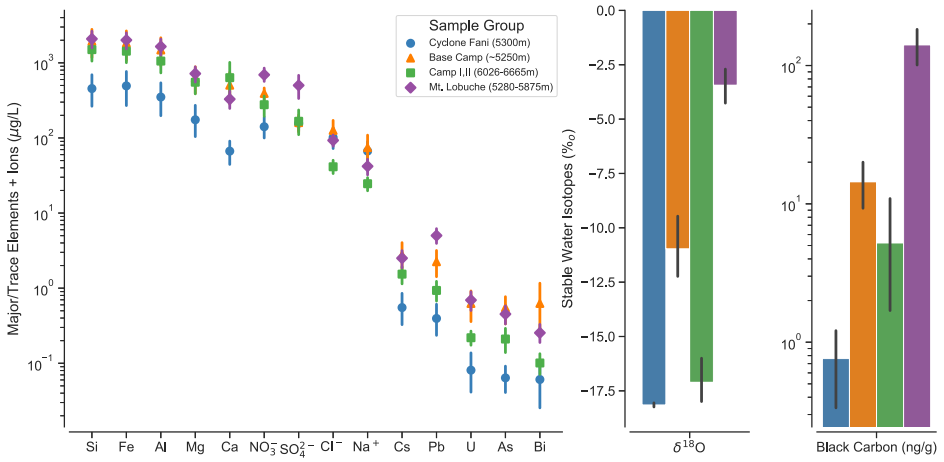


Fig. 3. Snow Chemistry by Sample Group. Average total concentrations of selected chemistry to elucidate crustal- (Si, Fe, Al, Mg, Ca), marine (Na^+, Cl^-), anions (NO_3^-, SO_4^{2-}) and known anthropogenically influenced chemistry (Pb, U, As, Bi, Cs), from snow samples at Everest Base Camp (orange triangle, $n = 39$ samples), Everest Base Camp during Cyclone Fani (blue circle, $n = 24$ samples), Camps I and II (green square, n = 24 samples), and Mt. Lobuche (purple diamond, $n = 7$ samples) in ascending order of average total snow concentrations. Extended chemistry measurements are found in Supplementary Material. Isotopic differences in air mass tracer $\delta^{18}O$ and variations in concentration of black carbon are also shown for each sample group. All error bars show 95% confidence intervals.

coincident with Cyclone Fani (Perry et al., 2020). Average concentrations of selected chemistry in addition to black carbon and $\delta^{18}O$ for snow sample locations are shown in Fig. 3. Black carbon (commonly referred to as soot), a known toxin (Janssen et al., 2012), is used in this study to supplement the chemistry data and will be expanded upon in a future study. Additional chemistry measurements and statistical overviews including rare earth elements are included in the Supplementary Material (**Fig. S2, S5**; **Table S3, S5**).

Based on the entire collection of snow samples, the most abundant elements (>1% total concentration) are Si > Fe > Al > K > Mg > Ca > Ti > Na. The most abundant cation in the snow is Ca^{2+} (77% of total cation concentration) followed by $Mg^{2+} > Na^+ > K^+$, and the most abundant anion in the snow is NO_3^- (53% total anion concentration) followed by $SO_4^{2-} > Cl^-$. The average $\delta^{18}O$ values in surface snow vary considerably, ranging from −1.9 to −21‰ (avg. -13.3‰). The more depleted values associated with the Camp I, II, and Cyclone Fani samples (Fig. 3), are similar to those found in the Khumbu Glacier ice core (Fig. 2). Samples collected at Camp I and II have $\delta^{18}O$ values that are more depleted (−17.1 ± 2.6‰) compared with lower elevation snow samples, which is consistent with lower temperatures at higher elevations and lifting of air masses with consequent depletion (Wen et al., 2012).

High elevation sampling locations along the Khumbu Glacier (Camp I and Camp II; 6000–6700 m) are dominated by crustal source elements and ions with relatively low concentrations of marine source and pollution-sourced chemistry, including black carbon (5 ± 13 ng/g). Our results suggest lower pre-monsoon concentrations of anthropogenic and marine source chemistry at the higher elevation sampling sites on Mt. Everest's southern aspect, and instead, the chemistry is dominated by dust deposition. Similar crustal element associations are noted in other high altitude locations (>6000 m) in the Himalayas (Carrico et al., 2003). By comparison, samples collected at Everest Base Camp have the highest concentrations for Cl^-, Bi, and As while Mt. Lobuche has the highest concentrations for the remaining chemistry, shown in Fig. 3. Black carbon concentrations are significantly higher at Mt. Lobuche (128 ± 71 ng/g) compared with the other sample locations (11 ± 19 ng/g).

PCA results for snow chemistry reveal three prominent principal components (>5% variance) that makeup 83% of the chemistry's total variance (**Table S4**). $PC1_{snow}$ and 65% of the variance is dominated by crustal elements (e.g., Si, Fe, Al, Mg, Co, Cr, Li, V, K), similar to PC1 from the Khumbu Glacier ice core. The second principal component ($PC2_{snow}$) with 10% of the variance is associated with marine and potentially anthropogenic source chemistry (e.g., Cl^-, Na^+, B, S, SO_4^{2-}, NO_3^-, K^+), similar to $PC3_{snow}$ from the Khumbu Glacier ice core chemistry. With 8% of the variance, PC3 includes P, Na, and potential anthropogenically sourced chemistry (e.g., W, Bi, U, As, Pb, Cs) and is negatively related to Ca^{2+}, SO_4^{2-}, Mg^{2+}, S, K^+, and Ca, likely associated with local

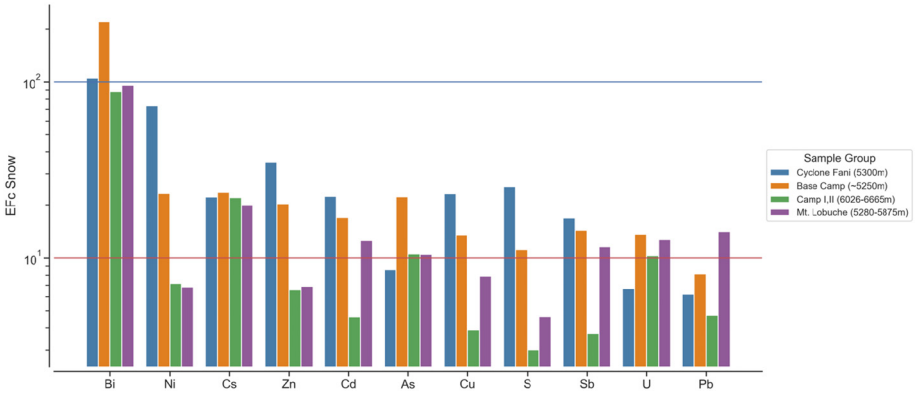


Fig. 4. Enrichment Factors of Snow. Enrichment factor values for snow (samples by location. Only elements with average EFc values > 10 for a sample group are shown for snow samples. Red horizontal line refers to EFc of 10 (enriched), blue line is EFc of 100 (highly enriched).

debris from rock weathering and mass wasting processes (Balestrini et al., 2014; Casey, 2012; Casey et al., 2012; Reynolds et al., 1995; Takeuchi et al., 2020).

To identify rock and soil dust in contrast to other potential sources, such as local or aeolian contaminants, we calculate the crustal enrichment factor (EFc) (Fig. 4) by taking the ratio of a selected metal to Al normalized to the mean upper continental crust ratio of the selected metal to Al (Ferrari et al., 2001; Wedepohl, 1986), averaging by each sample group, and removing outliers outside three times the standard deviation. An EFc below 10 suggests crustal sources are dominant, while an EFc greater than 10 signals the influence of additional (likely anthropogenic) sources, referred to in this study as "enriched" (Barbante et al., 2003; Ferrari et al., 2001; Halstead et al., 2000). The EFc values among the sample groups reveal enriched values for Bi, Ni, Cs, Zn, Cd, As, Cu, S, Sb, U, and Pb. EFc values for Bi in snow are highly enriched for all sample locations. High elevation sampling locations (Camp I and II) have fewer enriched elements (Bi, Cs, As) than lower elevation sites, indicating lesser anthropogenic influences. EFc values for Everest Base Camp show the largest number of enriched elements (Bi, Ni, Cs, Zn, Cd, As, S, Sb, U), consistent with the relatively large population residing at Everest Base Camp. Enriched Bi, Cs, Cd, As, Sb, U, and Pb are found in the Mt. Lobuche samples. Enriched values of Pb are only found in snow samples at Mt. Lobuche. Therefore, the anthropogenic signal is minor at higher elevation sites (Camp I and II) and more pronounced at Everest Base Camp and Mt. Lobuche. This is likely due to the decreased wind speed at lower elevations and higher deposition.

Airmass tracers, $\delta^{18}O$ (transport/atmospheric conditions), Si (crustal), Cl^- (marine), and Pb and Bi (anthropogenic) for the surface snow sampling period 2019/04/17 to 2019/05/10 is compared with hourly meteorological data from the Pyramid Weather Station (27.959°N, 86.813°E; 5035 m), located within ~6 km distance from Everest Base Camp (Fig. 5). Daily variations of Si, Bi, and Pb at Base Camp correspond with precipitation events. Concentrations decrease during and immediately after precipitation events, after which concentrations increase due to particulates accumulating after a snow event. Pb concentrations increase to >8 μg/L, five days after the April 23rd precipitation event and six days after the May 4th Cyclone Fani event. $\delta^{18}O$ values become more enriched from 17 to 21 April, then gradually become more depleted until 10 May at Everest Base Camp, except 1 May. Of the two days with highly enriched $\delta^{18}O$ values at Everest Base Camp (21 April, 1 May), $\delta^{18}O$ values at Mt. Lobuche are similarly enriched, collected on 1 May. The enriched $\delta^{18}O$ values (-3.4 ± 1.1‰) from Mt. Lobuche are linked with the sublimation of recent snow (Sokratov and Golubev, 2009) and melting on the surface.

Marine-sourced Na^+ is linked with precipitation events, with generally higher Na^+ concentrations immediately following precipitation events, and decreased concentrations during dry periods. Exceptionally high Na^+ concentrations were noted on 2 May at Base Camp, with no major preceding precipitation event, which could be associated with a crustal source based on Si's above-average values. The 4-day span of the collection at Camp I and II sites have consistently depleted $\delta^{18}O$ values and below-average Na^+ and Bi concentrations, with varying Si and Pb. Consistent with previous studies in the Himalayas, our results show that $\delta^{18}O$ values in surface snow decrease with elevation; based on the Base Camp, Camp I, and Camp II samples.

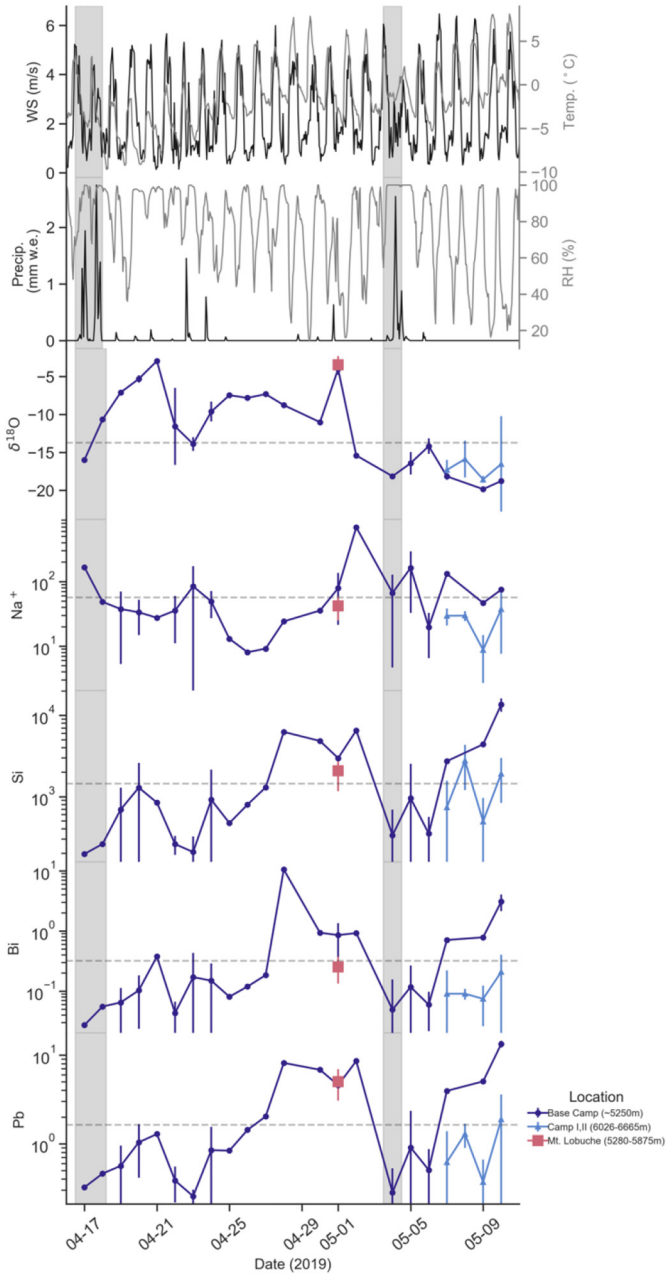


Fig. 5. Meteorological Data Compared with Atmospheric Tracers. Hourly meteorological data of wind speed (bold black) and temperature (gray); precipitation (bold black) and relative humidity (gray) from the Pyramid weather station (Sherpa et al., 2017) (27.959°N, 86.813°E; 5035 m;) for the duration of the sampling period (4/16 to 5/11) shown with $\delta^{18}O$ (‰), Na^+, Si, Bi, and Pb (μg/L) in surface snow for Everest Base Camp (dark blue circle), Camp I and II (light blue triangle), and Mt. Lobuche (red square), averaged by day, with error bars signifying 95% confidence intervals. Gray shading marks significant snow events with precip. >1.5 mm. Hourly data is based on local Nepal time or UTC + 5:45.

3.3. Cyclone Fani snow

We collected 24 snow samples from the largest snow accumulation event of the Khumbu sampling season, caused by Cyclone Fani that occurred from 3 May 17:00 to 4 May 22:00. Meteorological conditions during Cyclone Fani were characterized by 10.2 mm of total precipitation, average temperature of −0.4 °C, wind speed of 2.1 m/s, and relative humidity of 99.9%, from the Pyramid weather station (Fig. 5). Cyclone Fani is considered to be one of the strongest pre-monsoon cyclone events ever recorded in the Bay of Bengal and is unique due to its longevity, path, and timing (Mishra et al., 2020). To distinguish the path of Cyclone Fani, we used the Lagrangian particle dispersion model FLEXPART version 10.4 (Pisso et al., 2019) to explore moisture source regions associated with precipitation events at Phortse (27.85° N, 86.75° E). The model output presented in Fig. 6, shows the emission sensitivity (%) of 10,000 released inert tracer particles during the maturation hour of the Cyclone Fani storm event (5/3/2019 1600) over the previous 72-h. Resulting backward trajectories during Cyclone Fani exhibits similar features as the monsoon season (JJAS) backward trajectories from Perry et al. (2020), also noting sea surface temperatures in the

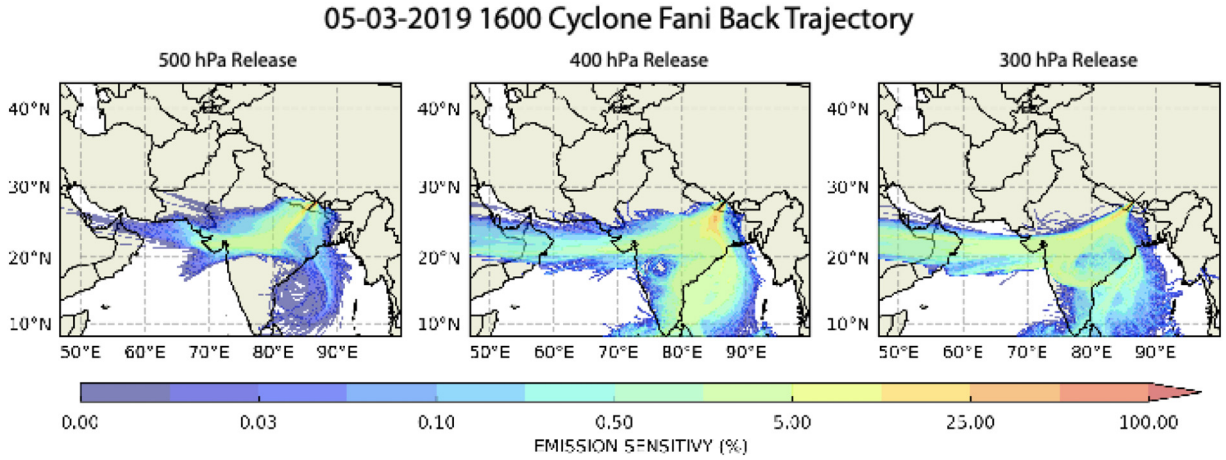


Fig. 6. Cyclone Fani Back Trajectories. Using Lagrangian particle dispersion model FLEXPART, showing the emission sensitivity (%) of 10,000 released inert tracer particles during the maturation hour of the Cyclone Fani storm event (5/3/2019 1600) over the previous 72-h from Phortse (27.85° N, 86.75° E) based on ERA5 reanalysis data at the 300, 400 and 500 hPa pressure level release. Refer to Supplementary Materials for further details about FLEXPART methodology. Figure created by Heather Guy.

Bay of Bengal as an important influence on precipitation rates in the Khumbu region. Moreover, the notable cyclone developed during a period of anomalously high sea surface temperature and high anthropogenic aerosol levels in the atmosphere above the Bay of Bengal (Zhao et al., 2020).

From the 24 Cyclone Fani snow samples, the resulting chemistry is characterized by elevated marine chemistry (Na^+, Cl^-, B, K^+) and sulfur (S, SO_4^{2-}), lower concentrations of crustal elements and black carbon, and consistently depleted $\delta^{18}O$ values compared with Everest Base Camp samples (Fig. 3, **S5**). In general, the pre-monsoon snow Na^+/Cl^- ratio (0.55 ± 0.2) is low compared with the seawater ratio (0.86). The Na^+/Cl^- ratio of Cyclone Fani is the highest of the snow samples groups (0.67 ± 0.1), and by comparison, is most similar to the Khumbu Glacier ice core and Khumbu Glacier melt streams (**Fig. S4**), therefore reflecting long-range transport of sea-salt source. The Cyclone Fani samples from Everest Base Camp are enriched in Bi, Ni, Cs, Zn, Cd, Cu, S, and Sb, and therefore likely from anthropogenic influences (Fig. 4).

3.4. Stream chemistry

We measured chemistry from six different locations (18 total), defined within this study as Khumbu Glacier melt-streams (KGM): KGM1 (5240 m) and KGM2 (5215 m); Khumbu Valley streams: Dughla (4820 m) and Pheriche (4320 m); and Imja Valley streams: Chukkung (4630 m) and Imja (5000 m) (Fig. 1, **Table S1**). These locations were chosen based on accessibility from the trekking path, location within the vicinity of local villages (Chukkung, Pheriche, Dughla), and closeness to the stream water source (KGM, Imja). Overall, stream sample concentrations are higher than snow and ice due to the combined influence of rock weathering, surface runoff, and glacier melt (Fig. 2). Pre-monsoon stream chemical concentrations are greater than those during the monsoon season, likely due to the dilution effect of monsoon precipitation (Raut et al., 2017).

For all stream measurements the most abundant elements (>1% total concentration) measured are Si > Fe > Al > Ca > K > Mg > Bi>S > Na > Mo. Ca^{2+} dominates stream waters at 82% of total cation concentration and SO_4^{2-} at 84% total anion concentration, followed by $Na^+ > K^+ > Mg^{2+}$ and $NO_3^- > Cl^-$, respectively. The stream $\delta^{18}O$ values are similar to the depleted snow values from Cyclone Fani and Camp I, II, while more enriched when compared to the ice core values. PCA results (**Table S4**) for the stream chemistry reflect crustal and anthropogenic sources. Crustal-sourced $PC1_{stream}$ (e.g., K, Si, Al, Fe) with 58% of the variance and $PC2_{stream}$ (e.g., S, Sr, Na^+, Ca^{2+}, SO_4^{2-}) with 25% of the variance are suggestive of silicate and carbonate and sulfate weathering (Balestrini et al., 2014; Reynolds et al., 1995), respectively. Potential anthropogenic source metals dominate $PC3_{stream}$ (7%) (e.g., Pb, Bi, As) and are negatively related to NO_3^-, Cl^-, and Ca^{2+}.

Average concentrations of selected chemistry for the six stream sample locations are shown in Fig. 7, including WHO drinking water safety level guidelines (WHO, 2017). Additional chemistry measurements and statistical overviews including rare earth elements are included in the Supplementary Material (**Fig. S2, S6**; **Table S3, S6**). $\delta^{18}O$ values from surface waters in the Khumbu and Imja Valley regions range from −15.1 to −18.4‰, whereas the Khumbu Glacier melt surface waters are more depleted (−17.3 to −21.7‰). The Khumbu Glacier melt stream samples from above Everest Basecamp (KGM1) exhibit the lowest concentrations for all chemical species, followed by the KGM2, reflecting proximity to glacial melt source and lack of geological material chemical signatures detected downstream. Samples, collected ~300 m downstream of the Imja Lake, exhibits the highest concentrations for Na^+, Mg^{2+}, SO_4^{2-}, Na, S, B, Mo and W. Highest average concentrations of crustal elements (e.g., Si, Fe, Al, Mg) are measured in the Chukkung samples, collected ~4.2 km downstream from the Imja Lake. Dughla stream samples, taken ~9 km downstream from KGM2 and 150 m north of the Dughla settlement, has the highest concentrations for K^+, Ca^{2+}, Ca, U, As, Sb, Sr, and Zn. About 5 km downstream from the Dughla sample, the Pheriche sample location has the highest concentrations of P, Pb, Bi, Ag, Cd, Cs, Cu, and Li, in addition to all rare earth elements. We note high enrichment factor calculations (>10) for Bi and Cs for all stream sample locations and within select locations, we calculate highly enriched U, S, Cs, As, Mo, and Pb (**Fig. S7).** For a more complete assessment of enrichment values, further sampling of sediments in addition to stream samples is recommended.

4. Discussion

4.1. Sources and points of interest

Concentrations of almost all chemistry measurements from ice cores, surface snow, and snowpits in previous studies have shown higher pre-monsoon concentrations than those during the monsoon season (Kang et al., 2007; Kaspari et al., 2014; Lee et al., 2008). Overall highest atmospheric dust loading occurs during the late pre-monsoon season, with more substantial contributions from the Taklamakan desert and southern Tibetan Plateau, and additional transport from North Africa, the Arabian Peninsula, Iran's arid regions, Pakistan, Afghanistan, and the Indian sub-continent (Duchi et al., 2014). Based on the snow chemistry, the influx of pre-monsoon dust deposition in the Khumbu region is strongly dominated by Si, Fe, Al, K, and Mg, reflected in PC1 of the snow chemistry. We find elevated Fe, Al, and

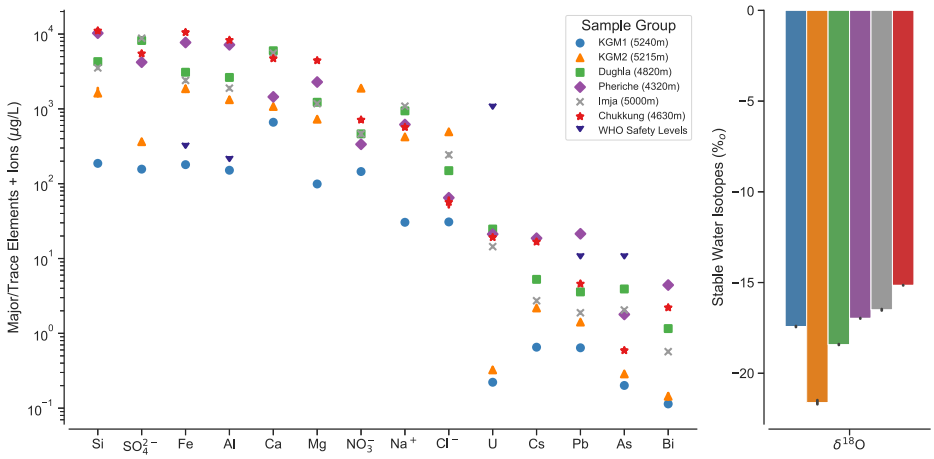


Fig. 7. Stream Chemistry by Sample Group. Average total concentrations of selected chemistry, specifically air mass tracer $\delta^{18}O$, crustal (Si, Fe, Al, Mg, Ca), marine (Na^+, Cl^-), anions (NO_3^-, SO_4^{2-}) and known anthropogenically influenced chemistry (Pb, U, As, Bi, Cs), from stream samples from Khumbu Glacier melt streams: KGM1 (light blue circle, n = 3), KGM2 (orange triangle, n = 3); Khumbu Valley streams: Dughla (green square, n = 3), Pheriche (purple diamond, n = 3); Imja Valley streams: Imja (gray 'x', n = 3), Chukkung (red star, n = 3). Drinking water safety level guidelines are included as dark blue downward facing triangle for reference (WHO, 2017). Extended chemistry measurements are found in Supplementary Material. All error bars show 95% confidence intervals.

Mg concentrations and reduced Ca and Na in our snow samples comparatively to prior studies in the region, summarized in **Table S7**. This could be due to our sampling timeframe during the pre-monsoon season.

Marine sourced chemistry, as demonstrated by $PC2_{snow}$ (e.g., Cl^-, Na^+, B, K^+), during the pre-monsoon season can reflect regional sources (e.g., Bay of Bengal, Arabian Sea) (Kaspari et al., 2007; Ming et al., 2007; Perry et al., 2020), and potentially more distant westerly sources (e.g., Mediterranean Sea) (Shrestha et al., 2002). Dominated by marine-sourced chemistry, Cyclone Fani has a similar chemical signature to the monsoon period, reflecting southerly sources based on back trajectories (Fig. 6). To investigate apparent differences in chemical signatures between monsoon (dominated by southerly air masses) and pre-monsoon (dominated by westerly air masses) atmospheric deposition, we observe the ratios in snow chemistry between Cyclone Fani and Everest Base Camp. Ratios >0.5 for Mo, SO_4^{2-}, Na^+, S, Cl^-, K^+, B, and Zn suggest a stronger contribution of southerly air masses rather than local/westerly sources. Prior precipitation data in the Mt. Everest region also shows higher Mo and Zn concentrations during the monsoon, similar to our findings (Cong et al., 2015), as well as in nearby alpine surface waters (Raut et al., 2017).

The Cyclone Fani signature is similar to $PC2_{snow}$, which is dominated by marine source chemistry (Cl^-, Na^+) and comparable to $PC3_{ice}$ from the Khumbu Glacier ice core (**Table S4**). The comparable signature exhibited by Cyclone Fani snow samples and the Khumbu Glacier ice core likely reflect the monsoon season captured within the ice core, also signified by the proximity of Na^+/Cl^- ratios (closest to 0.86, seawater) and depleted $\delta^{18}O$ values. The lower Na^+/Cl^- ratios, detected at Mt. Lobuche (**Fig. S4**), compared with seawater (excess Cl^-) could be due to the scavenging of atmospheric HCl (Shrestha et al., 1997, 2002), which has been found in fresh snow and snow pits in the northern Mt. Everest region (Kang et al., 2004; Shrestha et al., 2002), in addition to fresh snow from Cho Oyu in Tibet, about 25 km north-west of Mt. Everest (Balerna et al., 2003).

Comparison of EFc values from Everest Base Camp and snow collected after Cyclone Fani shows that snow deposited during Cyclone Fani is similarly enriched in anthropogenic source elements as Everest Base Camp. However, concentrations are much lower in the Cyclone Fani snow samples. This suggests a similar source for the anthropogenically enriched aerosols, but Cyclone Fani chemistry is likely diluted more effectively en route due to the high precipitation associated with this event. It's also likely that the aerosols are being diluted in the higher snow amounts, due to a flux effect.

The non-marine and non-crustal source chemistry associated with $PC2_{snow}$ (S, SO_4^{2-}, NO_3^-) is attributed to anthropogenic source aerosols since this association is not found in the pre-modern period Khumbu Glacier ice core samples. This signature's relationship with marine airmasses could reflect their chemical behavior with sea-salts in wet precipitation and co-emission of their precursors (i.e., SO_2 and NO_x) from anthropogenic emissions (Liu et al., 2013). Previous work in the Himalayas suggests that anions such as SO_4^{2-} and NO_3^- in precipitation are likely derived from regional anthropogenic sources including brick kilns, emissions from industry and agriculture, vehicle emissions, and dung combustion for heating (Li et al., 2007; Tripathee et al., 2014b, 2020). K^+, which is also prevalent in $PC2_{snow}$, is also derived from biomass burning.

Overall, the highest concentrations of heavy metals (e.g., Pb, Cs, Bi) and black carbon, in addition to the most enriched elements, were detected in the Everest Base Camp and Mt. Lobuche samples. We find higher average concentrations of anthropogenic chemistry (Pb, Cs, U, As, Bi) in our samples compared to several remote locations including the Arctic, Antarctic, Pamir mountains, and northern Tibetan Plateau, but lower concentrations than in more populated urban areas such as Kathmandu and Hong Kong (**Table S7**). Bi emerges as a significant pollutant with an average enriched value of ~100 in snow. High EFc values in Bi have been previously reported in surface snow (~30) from Mt. Everest's northeastern slope (Lee et al., 2008), a Miaoergou ice core (~400) from the eastern Tien Shan (Liu et al., 2011), on the Khumbu Glacier (~100) and nearby Ngozumpa glacier (~70)(Casey, 2012). While enriched Pb is only detected in the Mt. Lobuche samples, high concentrations of Pb are found in eight snow samples from Mt. Lobuche and Everest Base Camp (5–14 μg/L), approaching or exceeding the World Health Organization (WHO) drinking level standards (10 μg/L; WHO, 2017).

While we are unable to identify fixed source locations for anthropogenic source regions, we ran 36-h duration back trajectories for April 28 and May 2, 2019 (**Fig. S8**) where we observe high Bi and Pb, respectfully, in the Everest Base Camp samples (Fig. 5). The back trajectories indicate western sources, across Nepal and India, for both pollutants, however slightly varying trajectories such that April 28th (high Bi) has a more northern, westerly trajectory around 29° and 30° N and May 2nd (high Pb) has a more southern trajectory around 25° N. Our findings show there may be distinct provenances for different chemical species, however further research is necessary to further distinguish the sources of chemical signatures.

Black carbon measurements have a statistically significant ($p < 0.05$) positive correlation ($r > 0.8$) with Ag, Na, Pb, Zn, and Cu when grouped by daily averages for sample days (4/18–5/10) suggesting associated transport and deposition. Black carbon concentrations in the Khumbu are higher at elevations <6000 m, likely due to post-depositional processes including melt and sublimation, in addition to greater deposition at lower elevations (Kaspari et al., 2014). Accumulation of aerosols on the snow between precipitation events could also be responsible for higher concentrations of chemicals. Beyond the human health implications, high concentrations of impurities, including dust and black carbon, can decrease the albedo and increase snow/ice melt (Bonasoni et al., 2010; Jacobi et al., 2015; Kaspari et al., 2014; Yasunari et al., 2010).

The East Rongbuk Glacier ice core, collected from the north side of Mt. Everest (6500 m) and dated from 1650 to 2002 CE, is used to compare our measurements for further support of pre-modern concentrations (Fig. 2**, S1**). An increase in anthropogenic activities post-1950 is noted based on increased concentrations of Bi, U, Cs, Ca, and S (Kaspari et al., 2009b). We compare two-time frames from the East Rongbuk ice core, before (1650–1950) and after 1950 (1950–2002), where most selected elemental concentrations are higher than values obtained from the Khumbu Glacier ice core and below-average snow concentrations, with the exceptions of S and U. The comparison demonstrates the northern side of Mt. Everest is more susceptible to crustal and anthropogenic aerosol deposition, while the southern side has elevated levels of S and U, which could be due to distinct local geology (Kaspari et al., 2009b; Rengarajan et al., 2006) and/or atmospheric deposition (Balestrini et al., 2016; Cong et al., 2010a, 2009). In general, the Khumbu Glacier ice core chemistry is similar in composition to pre-modern levels measured in the East Rongbuk Glacier ice core, demonstrating an increase in anthropogenic pollution during the modern period (Kaspari et al., 2009b).

Based on the PCA results for the stream data, the most dominant influences on the chemistry is the local geology of the Khumbu and Imja stream locations, most likely silicate, carbonate, and sulfate weathering (Balestrini et al., 2014; Reynolds et al., 1995; Wood et al., 2020). Compared to the other streams sampled, the upper Khumbu Glacier melt stream (KGM1) concentrations are lowest, followed by the lower Khumbu Glacier melt stream (KGM2) except for NO_3^- and Cl^-, indicating a lesser influence from chemical weathering (Fig. 7**)**. Similar $\delta^{18}O$ values of KGM2 to the Khumbu Glacier ice core also suggest a stronger influence of snow/ice melt (Wood et al., 2020). More enriched $\delta^{18}O$ values in the Imja Valley streams could be from evaporation losses (Biggs et al., 2015) due to their origin from a large glacial lake sourced from Imja Glacier melt. The Khumbu and Imja Valley samples exhibit similar concentrations for crustal elements, while the Pheriche location has higher concentrations for anthropogenically sourced chemistry (Pb, Cs, Bi, Cd, Ag, Cu). We note somewhat elevated concentrations of crustal elements (Si, Fe, Al) and considerably higher concentrations in several anthropogenic elements (Pb, Cs, U) in comparison to surface waters in the broader region of Nepal (**Table S7**).

Concentrations of Na^+ and Cl^- in KGM streams are likely from long-range transport of sea-salt and ice melt based on their similarity to the average Na^+/Cl^- of 0.92 (seawater: 0.86). Average ratios from the Imja (4.5), Chukkung (10.4), Dughla (6.3), and Pheriche (9.6) samples signify an additional crustal source for Na^+, also indicated by a previous study with a ratio of 10.5 from Khumbu Valley streams (Balestrini et al., 2014) (**Fig. S4).** Anthropogenic influences in the stream samples are reflected in PC3 (7% variance) dominated by anthropogenic-source metals (Pb, Bi, As) and enriched EFc values of Bi, U, S, Cs, As, Mo, and Pb **(**Fig. 4**).** Enriched values in KGM streams likely reflect long-distance transport of anthropogenic aerosols deposited on the Khumbu Glacier. Although there are few studies on the chemical composition of streams or lake water from the high Himalayas, a previous study of alpine lake elemental chemistry in Nepal indicates enriched values of As, Ag, Mo, Zn, and Pb (Raut et al., 2017), similar to our study.

4.2. Watershed pollution implications

The recent Hindu Kush Himalaya assessment (Saikawa et al., 2019) identifies pollution as an increasingly severe threat to biodiversity, ecosystems, and human well-being, demonstrating the need for more extensive research regarding pollution in remote regions (Miner et al., 2020). Of the enriched elements measured in snow and streams in this study, most (Bi, U, As, Pb, Ni, Cs, Zn, Cd, Sb, Cu, S, Mo) are attributed to the long-range transport of aerosols from human sources (Nriagu, 1989; Pacyna and Pacyna, 2001). These are considered to be anthropogenically sourced in other Himalayan studies of snow and ice (Casey, 2012; Cong et al., 2010a; Dong et al., 2015; Gabrielli et al., 2020; Kaspari et al., 2009b; Lee et al., 2008; Tripathee et al., 2014a). Ice core records from the north side of Mt. Everest demonstrates that Bi, U, Cs, S, As, and Sb increased since the 1950s due to anthropogenic activities (Hong et al., 2009; Kaspari et al., 2009b), which has a similar chemical composition to that of the Khumbu Glacier ice core.

To assess the potential health risks associated with the water from the Khumbu region, we compare the major and trace element concentrations to safety guidelines. High concentrations of U (14–26 μg/L), approaching WHO safety guidelines (30 μg/L; WHO, 2017) are evident in streams sampled at Pheriche, Chukkung, Dughla, and Imja sampling sites, but not in stream samples KGM 1 and 2. High concentrations of U have been noted in glacier meltwater streams from the Khumbu (Reynolds et al., 1995) and are most likely sourced from chemical rock weathering, from local limestone, gypsum, or dolomite (Dossi et al., 2007). Based on WHO safety guidelines, the concentrations of Fe and Al at all stream sampling sites, except the Khumbu Glacier melt stream, exceed safe levels, although they are likely associated with natural processes (weathering and erosion) and land usage (Jenkins et al., 1995; Reynolds et al., 1995). Recent studies suggest climate change could contribute to increased weathering, melting permafrost, and falling water tables associated with rising metals and ions in watersheds (Manning et al., 2013; Todd et al., 2012).

Anthropogenic influences are evident at some stream sample locations, most noticeably in the Khumbu Valley streams at the Pheriche site. We find high Pb concentrations (21.4 ± 0.6 μg/L) at the Pheriche sampling site (Fig. 8), which is more than double the WHO safety level Pb value of 10 μg/L (WHO, 2017). We observe a significant 500% increase in average Pb concentrations from the Dughla to Pheriche sample locations (about 5 km apart), in addition to greater than 200% in other metal concentrations (Bi, Cs, Cu, Ag, Th, Sc, Mn). Although several studies on heavy metals in the region have not detected concerning levels of Pb in surface waters (Ghimire et al., 2014; Paudyal et al., 2016; Reynolds et al., 1995), a 2012 study found Pb levels exceeding WHO guidelines in Gokyo lake water samples (Sharma et al., 2012). Long-range transport of pollutants during the monsoon season is noted as Pb's primary source in the Gokyo lakes (Sharma et al., 2012). Based on Pb's high concentrations and the significant increase between the Dughla and Pheriche sites, we suggest potential contamination caused by unknown human activity upstream of the Pheriche sampling site (Fig. 8). A secondary source of water inflow, not related to Khumbu Glacier melt, is also possible; however, further research is necessary to determine a source.

While trace metals have not been previously identified as a health concern in the Khumbu Valley stream systems (Chevallier et al., 2020; Ghimire et al., 2014; Reynolds et al., 1995), water quality is projected to decline with warming and increased human emissions (Ghimire et al., 2013a; Nicholson et al., 2016, 2019). We found elevated concentrations of NO_3^- and Cl^- in the KGM2 samples compared with the KGM1 samples, collected directly downstream and upstream, respectively, from Everest Base Camp (Fig. 7). One study suggests increased concentrations of TN-NO_3^- (total nitrogen as nitrate), among other parameters, were observed in a three-year-long lake study in the Sagarmatha National Park that may be linked to increases in human waste (Ghimire et al., 2013b). Likely, two-thirds of the local domestic water supply during the dry, pre-monsoon season comes from the

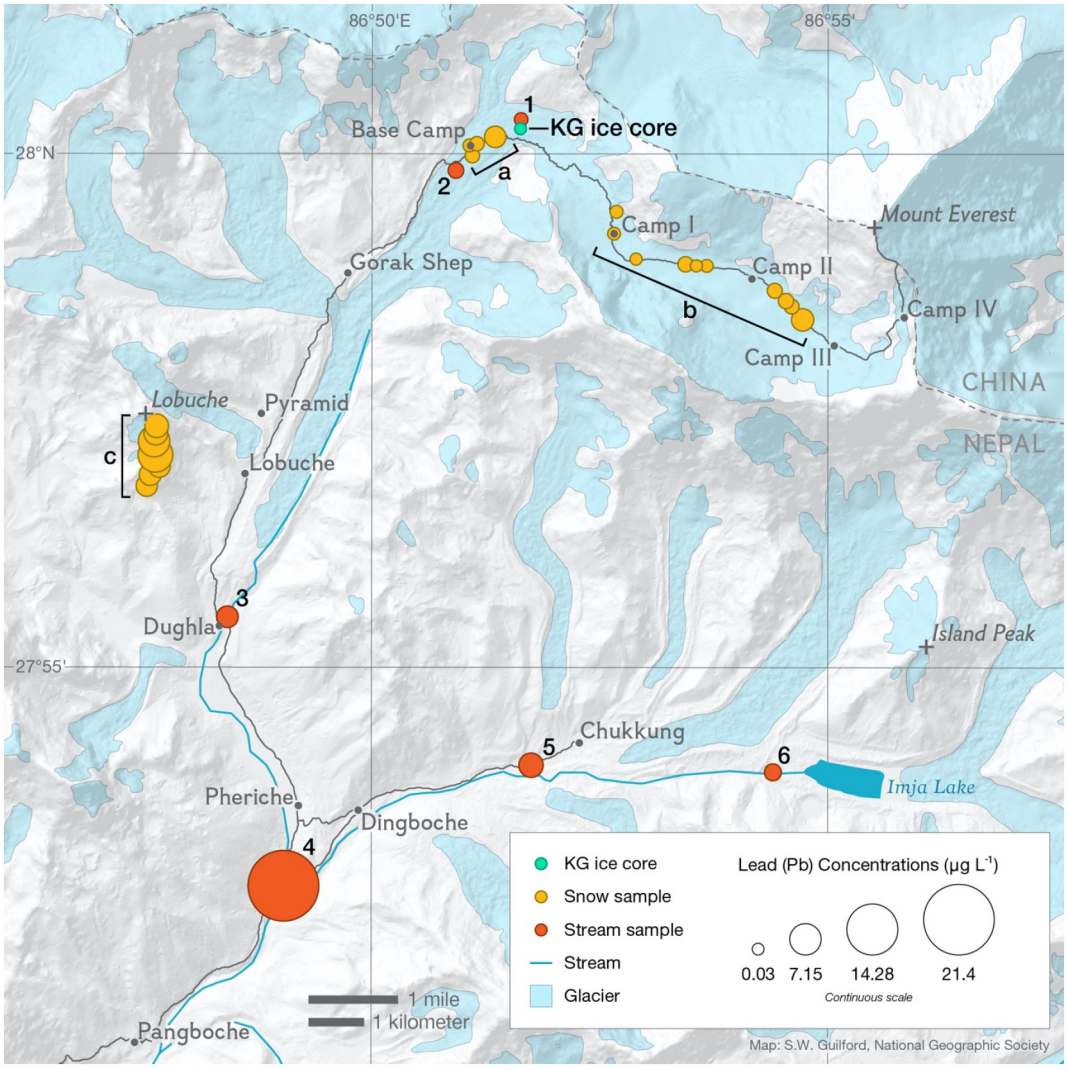


Fig. 8. Pb Concentrations by Sample Location. Shaded map of the regional area with location of snow (yellow), stream (red), and ice core samples (green), as well as the current glacial extent (aqua), stream paths (turquoise), and main trekking and climbing routes (gray). The size of each circle indicates Pb concentrations by location of sample in µg/L. Snow sample group locations identified as the following: a) Basecamp, b) Camp I,II, and c) Mt. Lobuche. Stream sample locations identified as the following: 1) KGM1, 2) KGM2, 3) Dughla, 4) Pheriche, 5) Chukkung, and 6) Imja. Glacial extent is sourced from the 2018 GLIMS glacier database (Raup et al., 2007), and polygons for the Everest area glaciers are extracted from the 2014 GLIMS dataset. Figure created by Sam Guilford.

meltwater of local glaciers such as the Khumbu Glacier (Wood et al., 2020). The local population of 3500–6000 people, in addition to the around 57,000 seasonal trekkers, climbers, and local support teams, depend on stream water derived from Khumbu Glacier melt for various purposes suggesting the need for future monitoring (Government of Nepal, 2020).

4.3. Directions for future research

This study, while beneficial, is limited by the number of samples collected and the timeframe of sampling. The Khumbu region would benefit from long-term, detailed monitoring of atmospheric and environmental chemistry to assess domestic water supply and potential sources of pollution. Rapid changes in glacier loss and precipitation (King et al., 2020; Perry et al., 2020), accumulation of chemicals and amplification of glacial melt from long-range transport of soot (Gul et al., 2021; Jacobi et al., 2015), and increased pressure on natural resources from the tourism industry (Aubriot et al., 2019; Chevallier et al., 2020; Wood et al., 2020) are just a few examples of current and future hazards in the Khumbu region. Tourism is of extreme economic importance in this area, so assuring the local environment is protected for long-term use is a priority. Because of the accessibility from tourism, further research on environmental chemistry in the Khumbu could be used as a guideline for other glaciated areas in the Himalayas impacted by trekkers or long-range pollutants. There is also the opportunity for researchers to partner with Sherpas and local villagers as a means of citizen science, which would allow them to be a part of the monitoring process in addition to valuing local knowledge (Sherpa et al., 2020).

For future monitoring of streams to be valuable, it would require continuous sampling for physical (e.g., pH, temperature, conductivity), chemical (e.g., major ions, trace elements measured here including Hg), and biological (e.g., coliform, *E. coli*) parameters (Ghimire et al., 2014, 2013a; Nicholson et al., 2016, 2019). While it would be most beneficial to collect samples year-round, the dry pre-monsoon season should be prioritized since it is less likely to be impacted by the precipitation dilution effect. Samples should be collected continuously from the same site locations, which should be spread out through the Khumbu and Imja regions to assess the impact of increasing population and elevation.

Further research on the transport and deposition of atmospheric chemistry in the Khumbu region would facilitate our understanding of source regions for different pollutants. A network of weather stations installed in different areas of the Khumbu (Phortse, Everest Basecamp, Camp II, South Col, Balcony) as part of our expedition in 2019 (Matthews et al., 2020) would pair well with continuous atmospheric measurements, as demonstrated by studies on pollutants (i.e., O_3 and black carbon) and atmospheric aerosol properties from the Nepal Climate Observatory (e.g., Bonasoni et al., 2010, 2008; Marcq et al., 2010; Sellegri et al., 2010; Yasunari et al., 2010). Based on our results, measuring heavy metals such as Pb and Bi, in addition to other trace elements, in the atmosphere and snow could help fingerprint anthropogenic pollutant source regions. Additionally, measuring the combination of elemental and mineralogical composition from snow samples could create an improved representation of the chemical and physical aerosol properties from diverse geographic locations and depositional environments (Alfonso et al., 2019; Cong et al., 2010a; Dong et al., 2016; Gao et al., 2018).

5. Conclusions

Here we present a comprehensive case study of surface snow, streams, and ice chemical composition in the Khumbu region. We identified major and trace elements, major ions, black carbon, and stable isotopes. Our findings document the 2019 pre-monsoon season, detailing chemistry from Cyclone Fani, spatial variability in snow and stream chemistry, and addressing potential pollution hazards. From snow chemistry, we find the pre-monsoon season is dominated by western air mass sources containing crustal elements and less frequent southerly marine air mass sources. The Khumbu and Imja Valley stream chemistry is strongly influenced by weathering and local geology, while Khumbu Glacier melt streams show strong correspondence to ice melt. Concerning concentrations of metals from natural and anthropogenic sources are found in Khumbu streams and warrant further research. We note that increased local tourism and land use are likely contributors to high metal concentrations in the stream samples. In addition, human waste at Everest Base Camp could be contributing to degraded water quality. Rising tourism in the Khumbu Valley and surrounding regions will likely contribute to greater pollutant loading, with important implications for the population of the Khumbu Valley who rely on this water source. With climate change and tourism increasing vulnerability in the Khumbu region, we find sufficient evidence of water quality degradation to suggest increased spatiotemporal environmental monitoring is needed in the Khumbu region.

CRediT authorship contribution statement

Heather M. Clifford: Conceptualization, Methodology, Writing – original draft, Writing – review & editing, Visualization, Investigation, Data curation, Formal analysis. **Mariusz Potocki:** Conceptualization, Methodology, Writing – review & editing, Visualization, Investigation. **Inka Koch:** Methodology, Writing – review & editing, Investigation. **Tenzing Sherpa:** Methodology, Writing – review & editing, Investigation. **Mike Handley:** Methodology, Investigation. **Elena Korotkikh:** Methodology, Investigation. **Douglas Introne:** Methodology, Investigation. **Susan Kaspari:** Methodology, Writing – review & editing, Investigation. **Kimberley Miner:** Writing – review & editing, Investigation. **Tom Matthews:** Writing – review & editing, Investigation. **Baker Perry:** Writing – review & editing, Investigation. **Heather Guy:** Visualization. **Ananta Gajurel:** Investigation. **Praveen Kumar Singh:** Methodology, Investigation. **Sandra Elvin:** Methodology, Writing – review & editing, Investigation, Resources. **Aurora C. Elmore:** Methodology, Writing – review & editing, Investigation, Resources. **Alex Tait:** Resources. **Paul A. Mayewski:** Methodology, Writing – original draft, Writing – review & editing, Investigation, Conceptualization, Supervision.

Declaration of competing interest

The authors declare that they have no known competing financial interests or personal relationships that could have appeared to influence the work reported in this paper.

Acknowledgments

This research was conducted through a partnership with the National Geographic Society, Rolex, and Tribhuvan University, with approval from all relevant agencies of the Government of Nepal. This work was supported by the National Geographic Society, Rolex, and NSF grant 1600018 (Mayewski). We wish to thank Shangri-La Nepal Trek Pvt. Ltd., Xtreme Climbers Treks and Expedition P. Ltd., the United States Embassy of Kathmandu, and the American Club, Conrad Anker, Pete Athans, Fisher Creative, and Virtual Wonders for all of their support. Many thanks to the National Geographic project staff and our fellow team members, and all of the porters, people, and businesses in the Khumbu Valley. We additionally acknowledge Margit Schwikowski and her team from the Paul Scherrer Institute, Villigen, Switzerland, for conducting ^{14}C measurements on the Khumbu Glacier ice core, and to Sam Guilford for providing figures. We would also like to acknowledge Patrick Wagnon from Univ. Grenoble Alpes, France for allowing us to use the weather station data from the Pyramid and Pheriche locations.

Appendix A. Supplementary data

Supplementary data to this article can be found online at https://doi.org/10.1016/j.scitotenv.2021.148006.

References

Alfonso, J.A., Cordero, R.R., Rowe, P.M., Neshyba, S., Casassa, G., Carrasco, J., MacDonell, S., Lambert, F., Pizarro, J., Fernandoy, F., Feron, S., Damiani, A., Llanillo, P., Sepulveda, E., Jorquera, J., Garcia, B., Carrera, J.M., Oyola, P., Kang, C.M., 2019. Elemental and mineralogical composition of the western Andean snow (18°S–41°S). Sci. Rep. 9, 1–13. https://doi.org/10.1038/s41598-019-44516-5.

Aubriot, O., Faulon, M., Sacareau, I., Puschiasis, O., Jacquemet, E., Smadja, J., André-Lamat, V., Abadia, C., Muller, A., 2019. Reconfiguration of the water-energy-food nexus in the Everest tourist region of Solukhumbu, Nepal. Mt. Res. Dev. 39, R47–R59. https://doi.org/10.1659/MRD-JOURNAL-D-17-00080.1.

Balerna, A., Bernieri, E., Pecci, M., Polesello, S., Smiraglia, C., Valsecchi, S., 2003. Chemical and radio-chemical composition of fresh snow samples from northern slopes of Himalayas (Cho Oyu range, Tibet). Atmos. Environ. 37, 1573–1581. https://doi.org/10.1016/S1352-2310(03)00009-8.

Balestrini, R., Polesello, S., Sacchi, E., 2014. Chemistry and isotopic composition of precipitation and surface waters in Khumbu valley (Nepal Himalaya): N dynamics of high elevation basins. Sci. Total Environ. 485–486, 681–692. https://doi.org/10.1016/j.scitotenv.2014.03.096.

Balestrini, R., Delconte, C.A., Sacchi, E., Wilson, A.M., Williams, M.W., Cristofanelli, P., Putero, D., 2016. Wet deposition at the base of Mt Everest: seasonal evolution of the chemistry and isotopic composition. Atmos. Environ. 146, 100–112. https://doi.org/10.1016/j.atmosenv.2016.08.056.

Barbante, C., Boutron, C., Morel, C., Ferrari, C., Jaffrezo, J.L., Cozzi, G., Gaspari, V., Cescon, P., 2003. Seasonal variations of heavy metals in central Greenland snow deposited from 1991 to 1995. J. Environ. Monit. 5, 328–335. https://doi.org/10.1039/b210460a.

Biggs, T.W., Lai, C.T., Chandan, P., Lee, R.M., Messina, A., Lesher, R.S., Khatoon, N., 2015. Evaporative fractions and elevation effects on stable isotopes of high elevation lakes and streams in arid western Himalaya. J. Hydrol. 522, 239–249. https://doi.org/10.1016/j.jhydrol.2014.12.023.

Bolch, T., Kulkarni, A., Kääb, A., Huggel, C., Paul, F., Cogley, J.G., Frey, H., Kargel, J.S., Fujita, K., Scheel, M., Bajracharya, S., Stoffel, M., 2012. The state and fate of himalayan glaciers. Science. 336 (6079), 310–314. https://doi.org/10.1126/science.1215828.

Bollasina, M., Bertolani, L., Tartari, G., 2002. Meteorological observations at high altitude in the Khumbu Valley, Nepal Himalayas, 1994-1999. Bull. Glaciol. Res. 19, 1–11.

Bonasoni, P., Laj, P., Angelini, F., Arduini, J., Bonafè, U., Calzolari, F., Cristofanelli, P., Decesari, S., Facchini, M.C., Fuzzi, S., Gobbi, G.P., Maione, M., Marinoni, A., Petzold, A., Roccato, F., Roger, J.C., Sellegri, K., Sprenger, M., Venzac, H., Verza, G.P., Villani, P., Vuillermoz, E., 2008. The ABC-Pyramid Atmospheric Research Observatory in Himalaya for aerosol, ozone and halocarbon measurements. Sci. Total Environ. 391, 252–261. https://doi.org/10.1016/j.scitotenv.2007.10.024.

Bonasoni, P., Laj, P., Marinoni, A., Sprenger, M., Angelini, F., Arduini, J., Bonafè, U., Calzolari, F., Colombo, T., Decesari, S., Di Biagio, C., Di Sarra, A.G., Evangelisti, F., Duchi, R., Facchini, M.C., Fuzzi, S., Gobbi, G.P., Maione, M., Panday, A., Roccato, F., Sellegri, K., Venzac, H., Verza, G.P., Villani, P., Vuillermoz, E., Cristofanelli, P., 2010. Atmospheric

Brown clouds in the Himalayas: first two years of continuous observations at the Nepal Climate Observatory-Pyramid (5079 m). Atmos. Chem. Phys. 10, 7515–7531. https://doi.org/10.5194/acp-10-7515-2010.
Bonasoni, P., Cristofanelli, P., Marinoni, A., Vuillermoz, E., Adhikary, B., 2012. Atmospheric pollution in the Hindu Kush–Himalaya region. Mt. Res. Dev. 32, 468–479. https://doi.org/10.1659/mrd-journal-d-12-00066.1.
Carrico, C.M., Bergin, M.H., Shrestha, A.B., Dibb, J.E., Gomes, L., Harris, J.M., 2003. The importance of carbon and mineral dust to seasonal aerosol properties in the Nepal Himalaya. Atmos. Environ. 37, 2811–2824. https://doi.org/10.1016/S1352-2310(03)00197-3.
Casey, K.A., 2012. Supraglacial dust and debris: geochemical compositions from glaciers in Svalbard, southern Norway, Nepal and New Zealand. Earth Syst. Sci. Data Discuss. 5, 107–145. https://doi.org/10.5194/essdd-5-107-2012.
Casey, K.A., Kääb, A., Benn, D.I., 2012. Geochemical characterization of supraglacial debris via in situ and optical remote sensing methods: a case study in Khumbu Himalaya, Nepal. Cryosphere 6, 85–100. https://doi.org/10.5194/tc-6-85-2012.
Chevallier, P., Seidel, J.L., Taupin, J.D., Puschiasis, O., 2020. Headwater flow geochemistry of Mount Everest (Upper Dudh Koshi River, Nepal). Front. Earth Sci. 8, 351. https://doi.org/10.3389/feart.2020.00351.
Cong, Z., Kang, S.C., Qin, D., 2009. Seasonal features of aerosol particles recorded in snow from Mt. Qomolangma (Everest) and their environmental implications. J. Environ. Sci. 21, 914–919. https://doi.org/10.1016/S1001-0742(08)62361-X.
Cong, Z., Kang, S., Dong, S., Liu, X., Qin, D., 2010a. Elemental and individual particle analysis of atmospheric aerosols from high Himalayas. Environ. Monit. Assess. 160, 323–335. https://doi.org/10.1007/s10661-008-0698-3.
Cong, Z., Kang, S., Zhang, Y., Li, X., 2010b. Atmospheric wet deposition of trace elements to central Tibetan Plateau. Appl. Geochem. 25, 1415–1421. https://doi.org/10.1016/j.apgeochem.2010.06.011.
Cong, Z., Kang, S., Zhang, Y., Gao, S., Wang, Z., Liu, B., Wan, X., 2015. New insights into trace element wet deposition in the Himalayas: amounts, seasonal patterns, and implications. Environ. Sci. Pollut. Res. 22, 2735–2744. https://doi.org/10.1007/s11356-014-3496-1.
Decesari, S., Facchini, M.C., Carbone, C., Giulianelli, L., Rinaldi, M., Finessi, E., Fuzzi, S., Marinoni, A., Cristofanelli, P., Duchi, R., Bonasoni, P., Vuillermoz, E., Cozic, J., Jaffrezo, J.L., Laj, P., 2010. Chemical composition of PM10 and PM1 at the high-altitude Himalayan station Nepal Climate Observatory-Pyramid (NCO-P) (5079 m a.s.l.). Atmos. Chem. Phys. 10, 4583–4596. https://doi.org/10.5194/acp-10-4583-2010.
Dixon, D.A., Mayewski, P.A., Korotkikh, E., Sneed, S.B., Handley, M.J., Introne, D.S., Scambos, T.A., 2011. A spatial framework for assessing current conditions and monitoring future change in the chemistry of the Antarctic atmosphere. Cryosphere Discuss. 5, 885–950. https://doi.org/10.5194/tcd-5-885-2011.
Dong, Z., Kang, S., Qin, X., Li, X., Qin, D., Ren, J., 2015. New insights into trace elements deposition in the snow packs at remote alpine glaciers in the northern Tibetan Plateau, China. Sci. Total Environ. 529, 101–113. https://doi.org/10.1016/j.scitotenv.2015.05.065.
Dong, Z., Qin, D., Kang, S., Liu, Y., Li, Y., Huang, J., Qin, X., 2016. Individual particles of cryoconite deposited on the mountain glaciers of the Tibetan Plateau: insights into chemical composition and sources. Atmos. Environ. 138, 114–124. https://doi.org/10.1016/j.atmosenv.2016.05.020.
Dossi, C., Ciceri, E., Giussani, B., Pozzi, A., Galgaro, A., Viero, A., Viganò, A., 2007. Water and snow chemistry of main ions and trace elements in the karst system of Monte Pelmo massif (Dolomites, Eastern Alps, Italy). Mar. Freshw. Res. 58, 649–656. https://doi.org/10.1071/MF06170.
Duan, J., Wang, L., Ren, J., Li, L., Han, J., 2009. Seasonal variations in heavy metals concentrations in Mt. Qomolangma Region snow. J. Geogr. Sci. 19, 249–256. https://doi.org/10.1007/s11442-009-0249-z.
Duchi, R., Cristofanelli, P., Marinoni, A., Bourcier, L., Laj, P., Calzolari, F., Adhikary, B., Verza, G.P., Vuillermoz, E., Bonasoni, P., 2014. Synoptic-scale dust transport events in the southern Himalaya. Aeolian Res. 13, 51–57. https://doi.org/10.1016/j.aeolia.2014.03.008.
Elvin, S., Athans, P., Mayewski, P., Ghimire, J., Elmore, A.C., Craig, V., 2020. Behind the scenes of a comprehensive scientific expedition to Mt. Everest. One Earth 3, 521–529. https://doi.org/10.1016/j.oneear.2020.10.006.
Fernández-Luqueño, F., López-Valdez, F., Gamero-Melo, P., Luna-Suárez, S., Aguilera-González, E., Martínez, A., García-Guillermo, M., Hernández-Martínez, G., Herrera-Mendoza, R., Álvarez-Garza, M., Pérez-Velázquez, I., 2013. Heavy metal pollution in drinking water - a global risk for human health: a review. Afr. J. Environ. Sci. Technol. 7, 567–584. https://doi.org/10.5897/AJEST12.197.
Ferrari, C.P., Clotteau, T., Thompson, L.G., Barbante, C., Cozzi, G., Cescon, P., Hong, S., Maurice-Bourgoin, L., Francou, B., Boutron, C.F., 2001. Heavy metals in ancient tropical ice: initial results. Atmos. Environ. 35, 5809–5815. https://doi.org/10.1016/S1352-2310(01)00347-8.
Gabrielli, P., Wegner, A., Roxana Sierra-Hernández, M., Beaudon, E., Davis, M., Barker, J.D., Thompson, L.G., 2020. Early atmospheric contamination on the top of the Himalayas since the onset of the European Industrial Revolution. Proc. Natl. Acad. Sci. U. S. A. 117, 3967–3973. https://doi.org/10.1073/pnas.1910485117.
Gao, Y., Yang, C., Ma, J., Yin, M., 2018. Characteristics of the trace elements and arsenic, iodine and bromine species in snow in east-central China. Atmos. Environ. 174, 43–53. https://doi.org/10.1016/j.atmosenv.2017.11.015.
Ghimire, N.P., Jha, P.K., Caravello, G., 2013a. Physico-chemical parameters of high-altitude rivers in the Sagarmatha (Everest) National Park, Nepal. J. Water Resour. Prot. 5, 761–767. https://doi.org/10.4236/jwarp.2013.58077.
Ghimire, N.P., Jha, P.K., Caravello, G., 2013b. Water quality of high-altitude lakes in the Sagarmatha (Everest) National Park, Nepal. J. Environ. Prot. 4, 22–28. https://doi.org/10.4236/jep.2013.47a003.
Ghimire, N.P., Shrestha, B.B., Jha, P.K., Caravello, G., 2014. Metals assessments in the water bodies of Sagarmatha National Park and buffer zone, Nepal. J. Water Resour. Prot. 6, 68–74. https://doi.org/10.4236/jwarp.2014.62011.
Government of Nepal, 2020. Nepal Tourism Statistics 2019 [WWW Document]. Minist. Cult. Tour. Civ. Aviat URL. https://www.tourism.gov.np/.
Grigholm, B., Mayewski, P.A., Kang, S., Zhang, Y., Morgenstern, U., Schwikowski, M., Kaspari, S., Aizen, V., Aizen, E., Takeuchi, N., Maasch, K.A., Birkel, S., Handley, M., Sneed, S., 2015. Twentieth century dust lows and the weakening of the westerly winds over the Tibetan Plateau. Geophys. Res. Lett. 42, 2434–2441. https://doi.org/10.1002/2015GL063217.
Gul, C., Mahapatra, P.S., Kang, S., Singh, P.K., Wu, X., He, C., Kumar, R., Rai, M., Xu, Y., Puppala, S.P., 2021. Black carbon concentration in the central Himalayas: impact on glacier melt and potential source contribution. Environ. Pollut. 275, 116544. https://doi.org/10.1016/j.envpol.2021.116544.
Halstead, M.J.R., Cunninghame, R.G., Hunter, K.A., 2000. Wet deposition of trace metals to a remote site in Fiordland, New Zealand. Atmos. Environ. 34, 665–676. https://doi.org/10.1016/S1352-2310(99)00185-5.
Hansen, J., Nazarenko, L., 2004. Soot climate forcing via snow and ice albedos. Proc. Natl. Acad. Sci. U. S. A. 101, 423–428. https://doi.org/10.1073/pnas.2237157100.
Hong, S., Lee, K., Hou, S., Soon, D.H., Ren, J., Burn, L.J., Rosman, K.J.R., Barbante, C., Boutron, C.F., 2009. An 800-year record of atmospheric As, Mo, Sn, and Sb in central Asia in high-altitude ice cores from Mt. Qomolangma (Everest), Himalayas. Environ. Sci. Technol. 43, 8060–8065. https://doi.org/10.1021/es901685u.
Immerzeel, W.W., Lutz, A.F., Andrade, M., Bahl, A., Biemans, H., Bolch, T., Hyde, S., Brumby, S., Davies, B.J., Elmore, A.C., Emmer, A., Feng, M., Fernández, A., Haritashya, U., Kargel, J.S., Koppes, M., Kraaijenbrink, P.D.A., Kulkarni, A.V., Mayewski, P.A., Nepal, S., Pacheco, P., Painter, T.H., Pellicciotti, F., Rajaram, H., Rupper, S., Sinisalo, A., Shrestha, A.B., Viviroli, D., Wada, Y., Xiao, C., Yao, T., Baillie, J.E.M., 2020. Importance and vulnerability of the world's water towers. Nature 577, 364–369. https://doi.org/10.1038/s41586-019-1822-y.
Jacobi, H.W., Lim, S., Ménégoz, M., Ginot, P., Laj, P., Bonasoni, P., Stocchi, P., Marinoni, A., Arnaud, Y., 2015. Black carbon in snow in the upper Himalayan Khumbu Valley, Nepal: observations and modeling of the impact on snow albedo, melting, and radiative forcing. Cryosphere 9, 1685–1699. https://doi.org/10.5194/tc-9-1685-2015.
Janssen, N.A., Gerlofs-Nijland, M.E., Lanki, T., Salonen, R.O., Cassee, F., Hoek, G., Fischer, P., Brunekreef, B., Krzyzanowski, M., 2012. Health Effects of Black Carbon. World Health Organization Regional Office for Europe, Copenhagen, Denmark.
Jenkins, A., Sloan, W.T., Cosby, B.J., 1995. Stream chemistry in the middle hills and high mountains of the Himalayas, Nepal. J. Hydrol. 166, 61–79. https://doi.org/10.1016/0022-1694(94)02600-G.
Jiao, X., Dong, Z., Kang, S., Li, Y., Jiang, C., Rostami, M., 2021. New insights into heavy metal elements deposition in the snowpacks of mountain glaciers in the eastern Tibetan Plateau. Ecotoxicol. Environ. Saf. 207, 111228. https://doi.org/10.1016/j.ecoenv.2020.111228.
Kang, S., Qin, D., Yao, T., Wake, C.P., Mayewski, P.A., 1999. Summer monsoon and dust signals recorded in the Dasuopu firn core, central Himalayas. Chin. Sci. Bull. 44, 2010–2015. https://doi.org/10.1007/BF02887130.
Kang, S., Mayewski, P.A., Qin, D., Yan, Y., Hou, S., Zhang, D., Ren, J., Kruetz, K., 2002. Glaciochemical records from a Mt. Everest ice core: relationship to atmospheric circulation over Asia. Atmos. Environ. 36, 3351–3361. https://doi.org/10.1016/S1352-2310(02)00325-4.
Kang, S., Mayewski, P.A., Qin, D., Sneed, S.A., Ren, J., Zhang, D., 2004. Seasonal differences in snow chemistry from the vicinity of Mt. Everest, central Himalayas. Atmos. Environ. 38, 2819–2829. https://doi.org/10.1016/j.atmosenv.2004.02.043.
Kang, S., Zhang, Q., Kaspari, S., Qin, D., Cong, Z., Ren, J., Mayewski, P.A., 2007. Spatial and seasonal variations of elemental composition in Mt. Everest (Qomolangma) snow/firn. Atmos. Environ. 41, 7208–7218. https://doi.org/10.1016/j.atmosenv.2007.05.024.
Kaspari, S., Mayewski, P., Kang, S., Sneed, S., Hou, S., Hooke, R., Kreutz, K., Introne, D., Handley, M., Maasch, K., Qin, D., Ren, J., 2007. Reduction in northward incursions of the South Asian monsoon since ~1400 AD inferred from a Mt. Everest ice core. Geophys. Res. Lett. 34, 1–6. https://doi.org/10.1029/2007GL030440.
Kaspari, S., Mayewski, P.A., Handley, M., Kang, S., Hou, S., Sneed, S., Maasch, K., Qin, D., 2009a. A high-resolution record of atmospheric dust composition and variability since A.D. 1650 from a Mount Everest ice core. J. Clim. 22, 3910–3925. https://doi.org/10.1175/2009JCLI2518.1.
Kaspari, S., Mayewski, P.A., Handley, M., Osterberg, E., Kang, S., Sneed, S., Hou, S., Qin, D., 2009b. Recent increases in atmospheric concentrations of Bi, U, Cs, S and Ca from a 350-year Mount Everest ice core record. J. Geophys. Res. Atmos. 114, 1–14. https://doi.org/10.1029/2008JD011088.
Kaspari, S., Painter, T.H., Gysel, M., Skiles, S.M., Schwikowski, M., 2014. Seasonal and elevational variations of black carbon and dust in snow and ice in the Solu-Khumbu, Nepal and estimated radiative forcings. Atmos. Chem. Phys. 14, 8089–8103. https://doi.org/10.5194/acp-14-8089-2014.
King, O., Quincey, D.J., Carrivick, J.L., Rowan, A.V., 2017. Spatial variability in mass loss of glaciers in the everest region, central Himalayas, between 2000 and 2015. Cryosphere 11, 407–426. https://doi.org/10.5194/tc-11-407-2017.
King, O., Bhattacharya, A., Ghuffar, S., Tait, A., Guilford, S., Elmore, A.C., Bolch, T., 2020. Six decades of glacier mass changes around Mt. Everest are revealed by historical and contemporary images. One Earth 3, 608–620. https://doi.org/10.1016/j.oneear.2020.10.019.
Lee, K., Hur, S. Do, Hou, S., Hong, S., Qin, X., Ren, J., Liu, Y., Rosman, K.J.R., Barbante, C., Boutron, C.F., 2008. Atmospheric pollution for trace elements in the remote high-altitude atmosphere in central Asia as recorded in snow from Mt. Qomolangma (Everest) of the Himalayas. Sci. Total Environ. 404, 171–181. https://doi.org/10.1016/j.scitotenv.2008.06.022.

Li, C., Kang, S., Zhang, Q., Kaspari, S., 2007. Major ionic composition of precipitation in the Nam Co region, Central Tibetan Plateau. Atmos. Res. 85, 351–360. https://doi.org/10.1016/j.atmosres.2007.02.006.

Liu, Y., Hou, S., Hong, S., Hur, S. Do, Lee, K., Wang, Y., 2011. High-resolution trace element records of an ice core from the eastern Tien Shan, central Asia, since 1953 AD. J. Geophys. Res. Atmos. 116, D12307. https://doi.org/10.1029/2010JD015191.

Liu, B., Kang, S., Sun, J., Zhang, Y., Xu, R., Wang, Y., Liu, Y., Cong, Z., 2013. Wet precipitation chemistry at a high-altitude site (3,326 m a.s.l.) in the southeastern Tibetan Plateau. Environ. Sci. Pollut. Res. 20, 5013–5027. https://doi.org/10.1007/s11356-012-1379-x.

Manning, A.H., Verplanck, P.L., Caine, J.S., Todd, A.S., 2013. Links between climate change, water-table depth, and water chemistry in a mineralized mountain watershed. Appl. Geochem. 37, 64–78. https://doi.org/10.1016/j.apgeochem.2013.07.002.

Marcq, S., Laj, P., Roger, J.C., Villani, P., Sellegri, K., Bonasoni, P., Marinoni, A., Cristofanelli, P., Verza, G.P., Bergin, M., 2010. Aerosol optical properties and radiative forcing in the high Himalaya based on measurements at the Nepal Climate Observatory-Pyramid site (5079 m a.s.l.). Atmos. Chem. Phys. 10, 5859–5872. https://doi.org/10.5194/acp-10-5859-2010.

Marinoni, A., Polesello, S., Smiraglia, C., Valsecchi, S., 2001. Chemical composition of freshsnow samples from the southern slope of Mt. Everest region (Khumbu-Himal region, Nepal). Atmos. Environ. 35, 3183–3190. https://doi.org/10.1016/S1352-2310(00)00488-X.

Marinoni, A., Cristofanelli, P., Laj, P., Duchi, R., Calzolari, F., Decesari, S., Sellegri, K., Vuillermoz, E., Verza, G.P., Villani, P., Bonasoni, P., 2010. Aerosol mass and black carbon concentrations, a two year record at NCO-P (5079 m, Southern Himalayas). Atmos. Chem. Phys. 10, 8551–8562. https://doi.org/10.5194/acp-10-8551-2010.

Matthews, T., Perry, L.B., Koch, I., Aryal, D., Khadka, A., Shrestha, D., Abernathy, K., Elmore, A.C., Seimon, A., Tait, A., Elvin, S., Tuladhar, S., Baidya, S.K., Potocki, M., Birkel, S.D., Kang, S., Sherpa, T.C., Gajurel, A., Mayewski, P.A., 2020. Going to extremes: installing the world's highest weather stations on Mount Everest. Bull. Am. Meteorol. Soc. https://doi.org/10.1175/BAMS-D-19-0198.1.

Mayewski, P.A., Pregent, G.P., Jeschke, P.A., Ahmad, N., 1980. Himalayan and Trans-Himalayan glacier fluctuations and the South Asian monsoon record. Arct. Alp. Res. 11, 171–182. https://doi.org/10.2307/1550514.

Mayewski, P.A., Lyons, W.B., Ahmad, N., 1983. Chemical composition of a high altitude fresh snowfall in the Ladakh Himalayas. Geophys. Res. Lett. 10, 105–108. https://doi.org/10.1029/GL010i001p00105.

Miner, K.R., Mayewski, P.A., Baidya, S.K., Broad, K., Clifford, H., Gajurel, A.P., Giri, B., Hubbard, M., Jaskolski, C., Koldewey, H., Li, W., Matthews, T., Napper, I., Perry, B., Potocki, M., Priscu, J.C., Tait, A., Thompson, R., Tuladhar, S., 2020. Emergent risks in the Mt. Everest region in the time of anthropogenic climate change. One Earth 3, 547–550. https://doi.org/10.1016/j.oneear.2020.10.008.

Ming, J., Zhang, D., Kang, S., Tian, W., 2007. Aerosol and fresh snow chemistry in the East Rongbuk Glacier on the northern slope of Mt. Qomolangma (Everest). J. Geophys. Res. Atmos. 112, 1–11. https://doi.org/10.1029/2007JD008618.

Mishra, S., Dwivedi, S.P., Singh, R.B., 2014. A review on epigenetic effect of heavy metal carcinogens on human health. Open Nutraceuticals J. 3, 188–193. https://doi.org/10.2174/1876396001003010018.

Mishra, S.P., Sethi, K.C., Ojha, A.C., Barik, K.K., 2020. Fani, an outlier among pre-monsoon intra-seasonal cyclones over Bay of Bengal. Int. J. Emerg. Technol. 11, 271–282.

Mohod, C.V., Dhote, J., 2013. Review of heavy metals in drinking water and their effect on human health. Int. J. Innov. Res. Sci. Eng. Technol. 2, 2992–2996.

Nicholson, K., Hayes, E., Neumann, K., Dowling, C., Sharma, S., 2016. Drinking water quality in the Sagarmatha National Park, Nepal. J. Geosci. Environ. Prot. 04, 43–53. https://doi.org/10.4236/gep.2016.44007.

Nicholson, K.N., Neumann, K., Dowling, C., Gruver, J., Sherman, H., Sharma, S., Sherma, H., Sharma, S., 2019. An assessment of drinking water sources in Sagarmatha National Park (Mt Everest region), Nepal. Mt. Res. Dev. 38, 353. https://doi.org/10.1659/mrd-journal-d-17-00024.1.

Nriagu, J.O., 1989. A global assessment of natural sources of atmospheric trace metals. Nature 338, 47–49. https://doi.org/10.1038/338047a0.

Osterberg, E.C., Handley, M.J., Sneed, S.B., Mayewski, P.A., Kreutz, K.J., 2006. Continuous ice core melter system with discrete sampling for major ion, trace element, and stable isotope analyses. Environ. Sci. Technol. 40, 3355–3361. https://doi.org/10.1021/es052536w.

Pacyna, J.M., Pacyna, E.G., 2001. An assessment of global and regional emissions of trace metals to the atmosphere from anthropogenic sources worldwide. Environ. Rev. 9, 269–298. https://doi.org/10.1139/er-9-4-269.

Paudyal, R., Kang, S., Sharma, C.M., Tripathee, L., Huang, J., Rupakheti, D., Sillanpää, M., 2016. Major ions and trace elements of two selected rivers near Everest region, southern Himalayas, Nepal. Environ. Earth Sci. 75, 1–11. https://doi.org/10.1007/s12665-015-4811-y.

Perry, L.B., Matthews, T., Guy, H., Koch, I., Khadka, A., Elmore, A.C., Shrestha, D., Tuladhar, S., Baidya, S.K., Maharjan, S., Wagnon, P., Aryal, D., Seimon, A., Gajurel, A., Mayewski, P.A., 2020. Precipitation characteristics and moisture source regions on Mt. Everest in the Khumbu, Nepal. One Earth 3, 594–607. https://doi.org/10.1016/j.oneear.2020.10.011.

Pisso, I., Sollum, E., Grythe, H., Kristiansen, N.I., Cassiani, M., Eckhardt, S., Arnold, D., Morton, D., Thompson, R.L., Groot Zwaaftink, C.D., Evangeliou, N., Sodemann, H., Haimberger, L., Henne, S., Brunner, D., Burkhart, J.F., Fouilloux, A., Brioude, J., Philipp, A., Seibert, P., Stohl, A., 2019. The Lagrangian particle dispersion model FLEXPART version 10.4. Geosci. Model Dev. 12, 4955–4997. https://doi.org/10.5194/gmd-12-4955-2019.

Pritchard, H.D., 2019. Asia's shrinking glaciers protect large populations from drought stress. Nature 569, 649–654. https://doi.org/10.1038/s41586-019-1240-1.

Raup, B., Racoviteanu, A., Khalsa, S.J.S., Helm, C., Armstrong, R., Arnaud, Y., 2007. The GLIMS geospatial glacier database: a new tool for studying glacier change. Glob. Planet. Chang. 56, 101–110. https://doi.org/10.1016/j.gloplacha.2006.07.018.

Raut, R., Bajracharya, R.M., Sharma, S., Sharma, C.M., Kang, S., Zhang, Q., Tripathee, L., Chen, P., Rupakheti, D., Guo, J., Dongol, B.S., 2017. Potentially toxic trace metals in water and lake-bed sediment of Panchpokhari, an alpine lake series in the Central Himalayan Region of Nepal. Water Air Soil Pollut. 228, 303. https://doi.org/10.1007/s11270-017-3467-5.

Rengarajan, R., Sarin, M.M., Krishnaswami, S., 2006. Dissolved uranium and 234U/238U in the Yamuna and the Chambal rivers, India. Aquat. Geochem. 12, 73–101. https://doi.org/10.1007/s10498-005-1421-4.

Reynolds, B., Chapman, P.J., French, M.C., Jenkins, A., 1995. Major, minor, and trace element chemistry of surface waters in the Everest region of Nepal. IAHS Publ. Proc. Reports-Intern Assoc Hydrol. Sci. 405–412.

Saikawa, E., Panday, A., Kang, S., Gautam, R., Zusman, E., Cong, Z., Somanathan, E., Adhikary, B., 2019. Air pollution in the Hindu Kush Himalaya. The Hindu Kush Himalaya Assessment. Springer International Publishing, pp. 339–387 https://doi.org/10.1007/978-3-319-92288-1_10.

Sellegri, K., Laj, P., Venzac, H., Boulon, J., Picard, D., Villani, P., Bonasoni, P., Marinoni, A., Cristofanelli, P., Vuillermoz, E., 2010. Seasonal variations of aerosol size distributions based on long-term measurements at the high altitude Himalayan site of Nepal Climate Observatory-Pyramid (5079 m), Nepal. Atmos. Chem. Phys. 10, 10679–10690. https://doi.org/10.5194/acp-10-10679-2010.

Sharma, C.M., Sharma, S., Bajracharya, R.M., Gurung, S., Jüttner, I., Kang, S., Zhang, Q., Li, Q., 2012. First results on bathymetry and limnology of high-altitude lakes in the Gokyo Valley, Sagarmatha (Everest) National Park, Nepal. Limnology 13, 181–192. https://doi.org/10.1007/s10201-011-0366-0.

Sherpa, S.F., Wagnon, P., Brun, F., Berthier, E., Vincent, C., Lejeune, Y., Arnaud, Y., Kayastha, R.B., Sinisalo, A., 2017. Contrasted surface mass balances of debris-free glaciers observed between the southern and the inner parts of the Everest region (2007-15). J. Glaciol. 63, 637–651. https://doi.org/10.1017/jog.2017.30.

Sherpa, T.C., Hubbard, M., Sherpa, P., Koch, I., Basukala, K., Timalsina, M., Athans, P., 2020. Voices from the roof of the world. One Earth 3, 518–520. https://doi.org/10.1016/j.oneear.2020.10.005.

Shichang, K., Kreutz, K.J., Mayewski, P.A., Qin, D., Yao, T., 2002. Stable-isotopic composition of precipitation over the northern slope of the central Himalaya. J. Glaciol. 48, 519–526. https://doi.org/10.3189/172756502781831070.

Shrestha, A.B., Wake, C.P., Dibb, J.E., 1997. Chemical composition of aerosol and snow in the high Himalaya during the summer monsoon season. Atmos. Environ. 31, 2815–2826. https://doi.org/10.1016/S1352-2310(97)00047-2.

Shrestha, A.B., Wake, C.P., Dibb, J.E., Whitlow, S.I., 2002. Aerosol and precipitation chemistry at a remote Himalayan site in Nepal. Aerosol Sci. Technol. 36, 441–456. https://doi.org/10.1080/027868202753571269.

Sokratov, S.A., Golubev, V.N., 2009. Snow isotopic content change by sublimation. J. Glaciol. 55, 823–828. https://doi.org/10.3189/002214309790152456.

Stone, E.A., Schauer, J.J., Pradhan, B.B., Dangol, P.M., Habib, G., Venkataraman, C., Ramanathan, V., 2010. Characterization of emissions from South Asian biofuels and application to source apportionment of carbonaceous aerosol in the Himalayas. J. Geophys. Res. Atmos. 115, 1–14. https://doi.org/10.1029/2009JD011881.

Takeuchi, N., Hori, Y., Furukawa, N., Yoshida, M., Fujii, Y., 2020. Glacio-environmental aspects recorded in two shallow ice cores drilled in 1980 at accumulation area of Khumbu Glacier of Mt. Everest in Nepal Himalayas. Arct. Antarct. Alp. Res. 52, 605–616. https://doi.org/10.1080/15230430.2020.1833681.

Tartari, G., Verza, G., Bertolami, L., 1998a. Meteorological data at the Pyramid Observatory Laboratory (Khumbu Valley, Sagarmatha National Park, Nepal). J. Limnol. 57, 23–40.

Tartari, G.A., Tartari, G., Mosello, R., 1998b. Water chemistry of high altitude lakes in the Khumbu and Imja Kola valleys (Nepalese Himalayas). J. Limnol. 57, 51–76.

Tchounwou, P.B., Yedjou, C.G., Patlolla, A.K., Sutton, D.J., 2012. Molecular, clinical and environmental toxicicology volume 3: environmental toxicology. Mol. Clin. Environ. Toxicol. 101, 133–164. https://doi.org/10.1007/978-3-7643-8340-4.

Thompson, L.G., Yao, T., Mosley-Thompson, E., Davis, M.E., Henderson, K.A., Lin, P.N., 2000. A high-resolution millennial record of the South Asian Monsoon from Himalayan ice cores. Science 289 (5486), 1916–1919. https://doi.org/10.1126/science.289.5486.1916.

Todd, A.S., Manning, A.H., Verplanck, P.L., Crouch, C., McKnight, D.M., Dunham, R., 2012. Climate-change-driven deterioration of water quality in a mineralized watershed. Environ. Sci. Technol. 46, 9324–9332. https://doi.org/10.1021/es3020056.

Tripathee, L., Kang, S., Huang, J., Sharma, C.M., Sillanpää, M., Guo, J., Paudyal, R., 2014a. Concentrations of trace elements in wet deposition over the central Himalayas, Nepal. Atmos. Environ. 95, 231–238. https://doi.org/10.1016/j.atmosenv.2014.06.043.

Tripathee, L., Kang, S., Huang, J., Sillanpää, M., Sharma, C.M., Lüthi, Z.L., Guo, J., Paudyal, R., 2014b. Ionic composition of wet precipitation over the southern slope of central Himalayas, Nepal. Environ. Sci. Pollut. Res. 21, 2677–2687. https://doi.org/10.1007/s11356-013-2197-5.

Tripathee, L., Kang, S., Li, C., Sun, S., Sharma, C.M., 2020. Chemical Components and Distributions in Precipitation in the Third Pole, Water Quality in the Third Pole. Elsevier Inc https://doi.org/10.1016/b978-0-12-816489-1.00001-3.

Uglietti, C., Zapf, A., Jenk, T.M., Sigl, M., Szidat, S., Salazar, G., Schwikowski, M., 2016. Radiocarbon dating of glacier ice: overview, optimisation, validation and potential. Cryosphere 10, 3091–3105. https://doi.org/10.5194/tc-10-3091-2016.

Valsecchi, S., Smiraglia, C., Tartari, G., Polesello, S., 1999. Chemical composition of monsoon deposition in the Everest region. Sci. Total Environ. 226, 187–199. https://doi.org/10.1016/S0048-9697(98)00393-3.

Wake, C.P., Mayewski, P.A., Spencer, M.J., 1990. A review of central Asian glaciochemical data. Ann. Glaciol. 14, 301–306. https://doi.org/10.3189/s026030550000879x.

Wake, C.P., Mayewski, P.A., Zichu, X., Ping, W., Zhongqin, L., 1993. Regional distribution of monsoon and desert dust signals recorded in Asian glaciers. Geophys. Res. Lett. 20, 1411–1414. https://doi.org/10.1029/93GL01682.

Wang, Y., Wu, N., Kunze, C., Long, R., Perlik, M., 2019. Drivers of change to mountain sustainability in the Hindu Kush Himalaya. The Hindu Kush Himalaya Assessment. Springer International Publishing, pp. 17–56 https://doi.org/10.1007/978-3-319-92288-1_2.

Wedepohl, K.H., 1986. Chapter 5: the composition of the continental crust. Int. Geophys. 34, 213–241. https://doi.org/10.1016/S0074-6142(09)60137-6.

Wen, R., Tian, L. De, Weng, Y.B., Liu, Z.F., Zhao, Z.P., 2012. The altitude effect of $\delta^{18}O$ in precipitation and river water in the southern Himalayas. Chin. Sci. Bull. 57, 1693–1698. https://doi.org/10.1007/s11434-012-4992-7.

WHO - World Health Organization, 2017. Guidelines for Drinking-water Quality. World Health Organization https://doi.org/10.1016/S1462-0758(00)00006-6.

Wood, L.R., Neumann, K., Nicholson, K.N., Bird, B.W., Dowling, C.B., Sharma, S., Wood, L.R., 2020. Melting Himalayan Glaciers Threaten Domestic Water Resources in the Mount Everest Region, Nepal. vol. 8, pp. 1–8. https://doi.org/10.3389/feart.2020.00128.

Yasunari, T.J., Bonasoni, P., Laj, P., Fujita, K., Vuillermoz, E., Marinoni, A., Cristofanelli, P., Duchi, R., Tartari, G., Lau, K.M., 2010. Estimated impact of black carbon deposition during pre-monsoon season from Nepal Climate Observatory - pyramid data and snow albedo changes over Himalayan glaciers. Atmos. Chem. Phys. 10, 6603–6615. https://doi.org/10.5194/acp-10-6603-2010.

Zhang, D., Qin, D., Hou, S., Kang, S., Ren, J., Mayewski, P.A., 2005. Climatic significance of $\delta^{18}O$ records from an 80.36 m ice core in the East Rongbuk Glacier, Mount Qomolangma (Everest). Sci. China Ser. D Earth Sci. 48, 266–272. https://doi.org/10.1360/02YD0219.

Zhao, L., Simon Wang, S.Y., Becker, E., Yoon, J.H., Mukherjee, A., 2020. Cyclone Fani: the tug-of-war between regional warming and anthropogenic aerosol effects. Environ. Res. Lett. 15. https://doi.org/10.1088/1748-9326/ab91e7.